GRAYSCALE LITHOGRAPTHY AND RESIST REFLOW FOR PARYLENE PATTERNING

Charmaine Chia and Joel Martis

Staff Mentors: Swaroop Kommera & Michelle Rincon

External Mentor: Michael Robles

JUNE 8, 2018

STANFORD UNIVERSITY

Contents

Introduction

1) Grayscale lithography
    - Introduction
    - Process flow
    - Characterization
2) Resist reflow studies
    - Motivation and applications
    - Physics of resist reflow
    - Experiments and analysis strategy
    - Profile data
    - Linear regression & Surface plots
    - Use case and Simulations
3) Quasi-liftoff of parylene
    - Process development
    - Patterning and etching
    - SEM imaging results

Concluding remarks

Acknowledgements

References

Appendix

1. Classification of number of lobes
2. Linear regression coefficients
3. Surface plots

Introduction

This project began with the goal of developing a quasi-liftoff process for parylene, which has wide ranging applications, including biomedical device design (which was part of the first author's PhD research). However, as with many research endeavors, we found a new avenue worth exploring (resist reflow), and a major chunk of time was devoted to studying and characterizing resist reflow. The goals of the project were thus broadened and detailed characterization of resist reflow was carried out with the hope that it would benefit the SNF community at Stanford.

This report has three main sections. The first section gives an overview of grayscale lithography, details on using the Heidelberg (SNF's grayscale lithography tool), and characterization of samples after grayscale lithography. The second section talks about resist reflow, namely, our motivation to study it, how we carried out experiments, and how we consolidated data in a form that would be useful to the SNF community. Grayscale lithography and thermal resist reflow are two ways of achieving non-vertical sidewalls on photoresist structures. The final section returns to the original goal of the project, quasi-liftoff of parylene, and elaborates on recipes developed with the help of knowledge gained in the first two sections of the report. Finally, the appendix lists all of the resist reflow data we gathered in a form that is useful to the user community at SNF.

I. Grayscale Lithography & Resist Characterization

Introduction

Traditional photolithography involves exposing selected regions of photoresist on a substrate, which after development gives rise to binary structures as shown in Fig 1. Certain applications, however, might require topological features on the substrate, thereby warranting the need to control exposure depth and obtain topographic features. This is precisely what grayscale lithography does, as shown in Fig 2.

Fig 2: Grayscale lithography on a positive photoresist

Process flow

Grayscale lithography involves all the steps present in traditional photolithography, with the addition of a few steps which are highlighted in blue here:

1. Choosing a resist
2. Obtaining the contrast curve

3. Preparing CAD files for grayscale lithography
4. Exposure
5. Development
6. Iterative optimization of grayscale doses (not covered here)

The above steps are elaborated below.

1. Choosing a resist

The choice of photoresist depends on the processes involved following lithography. Grayscale lithography, however, requires a photoresist that has a wide-range contrast curve for a given exposure tool in the nanofabrication facility. In our case, we chose the photoresist SPR 220-7 as its dose to clear matches the minimum base dose defined by the Heidelberg grayscale system, as well as requirements from our application in the quasi-liftoff of parylene.

2. Obtaining contrast curves

A contrast curve plots exposure depth (and hence, photoresist removed) versus radiation dose. This means that contrast curve is specific to the photoresist and lithography tool. Fig 3 shows some sample contrast curves; curve ‘b’ is ideal, while curves ‘a’ and ‘c’ are not because curve ‘a’ has a steep slope (i.e., lower grayscale resolution) and curve ‘c’ does not cover the full range of photoresist height. In addition to the dose, the Heidelberg also has another control parameter called the defocus value (ranging from 1 to 3) which can be used to control radiation exposure. A ‘dose-defocus’ exposure (Fig 4) enables the user to completely sweep the parameter space of the Heidelberg and conclude if the resist is suitable for the process, and obtain quantitative information on the dose required for specific exposures. In our case, we exposed a wafer to doses ranging from 0 mJ/cm^2 to 400 mJ/cm^2 in steps of 25 mJ/cm^2 (the maximum dose is 510 mJ/cm^2) and measured the resist remaining after development using the nanospec.

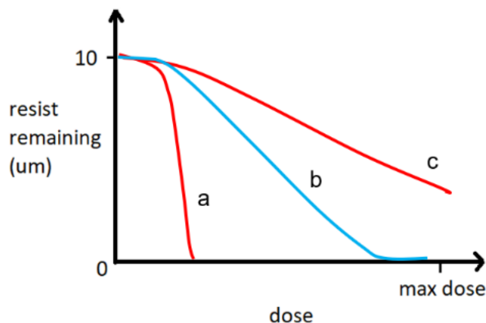

Fig 3: Contrast curves

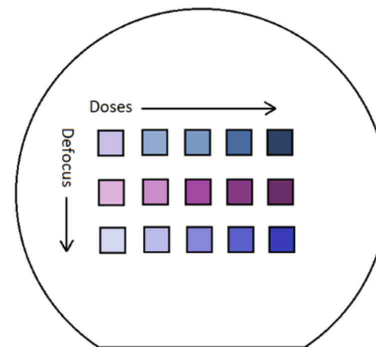

Fig 4: Dose-defocus exposure on a wafer

Fig 5 shows SPR220-7 contrast curves for different defocus values. The contrast curves cover the whole range of resist height (0-7um) and dose (0 - 510 mJ/cm^2). It is seen that the defocus value does not influence the contrast curves significantly for this resist.

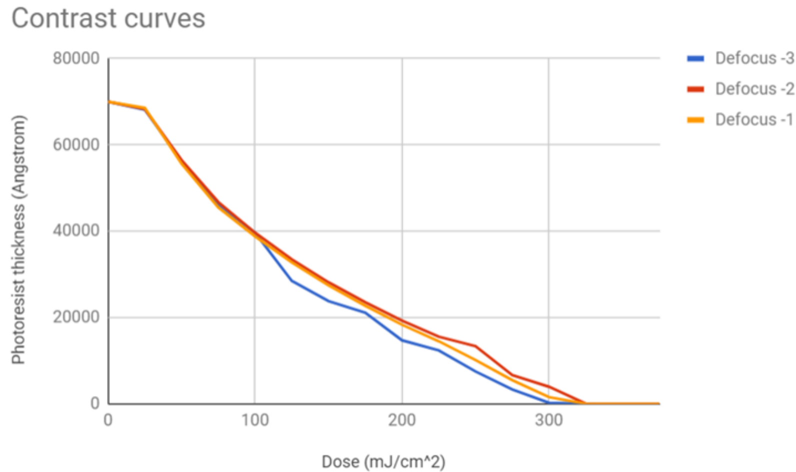

Fig 5: SPR 220-7 contrast curves

3. Preparing CAD files for grayscale lithography

A CAD file for grayscale lithography comprises of several layers, each layer corresponding to a different exposure value (Fig 6). For the Heidelberg, each layer must be a simple closed curve (Fig 7 illustrates the difference). The Heidelberg accepts .gds files as the primary file format for conversion into machine language. SNF has a computer area with desktops having full versions of Layout Editor (and equivalent software), which we used to prepare CAD files during the course of our project. Other CAD programs which could be used (and are available at SNF) are AutoCAD and LEdit.

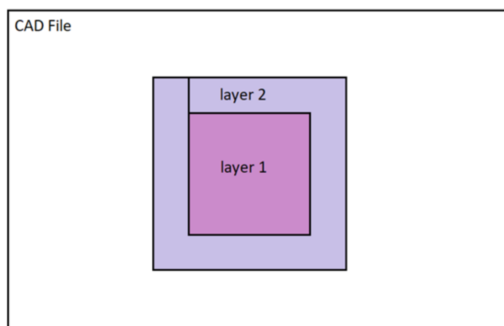

Fig 6: A sample CAD file with two exposure layers

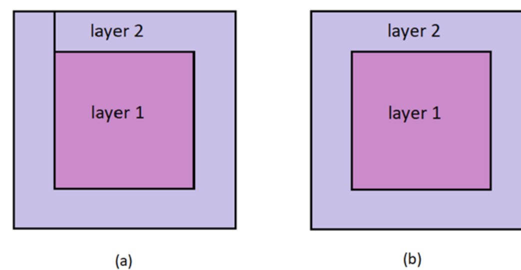

Fig 7: Examples of (a) acceptable and (b) non-acceptable CAD files (specific to the Heidelberg). In (a) both layers are closed polygons, and in (b) layer 2 is not a closed polygon

Fig 8 shows one of our CAD files in Layout Editor. The geometry consists of an 8x8 matrix of identical patterns, which constituted the individual splits, which will be discussed later. Each pattern has a 3x3 matrix of squares of different sizes (1000 um, 500 um, 100 um) and slopes (25°, 45°, 65°). The zoomed in view shows that each layer is a closed polygon.

4. Resist exposure

Patterning on the Heidelberg involves a number of steps, all of which are explained in detail in the user manual for the Heidelberg. In summary, once the wafer/chip is loaded onto the tool, one must load the CAD file and specify grayscale exposure values for different layers. The Heidelberg

has an 8 bit resolution for grayscale levels i.e., $2^8 = 256$ grayscale values, which range from 0 (no radiation) to 255 (maximum dose). The grayscale values for different layers must be calculated using the contrast curve. Since the grayscale levels are linear with actual dose, they can be calculated by simply finding the integer that most closely approximates actual dose to maximum (base) dose for a given layer. This is shown in Table 1 below, where we calculate grayscale values needed to fabricate a 7 layered square with 1 micron spacing between two layers.

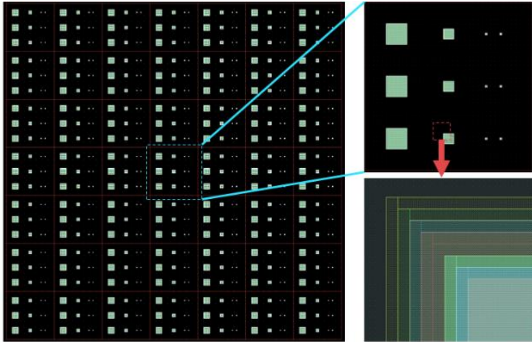

Fig 8: (clockwise from left) (i) CAD file with an 8x8 array of patterns for grayscale splits; (ii) pattern on a single piece (iii) edge of a square highlighting different layers, all of which are closed polygons

Layer	Resist remaining (um)	Dose (mJ/cm2)	Base dose (mJ/cm2)	% of base dose	Corresponding grey value	Actual grey value used
1	0	510	510	1.00	255	255
2	1	260	510	0.51	130	130
3	2	200	510	0.39	100	100
4	3	140	510	0.27	70	70
5	4	95	510	0.19	47.5	47
6	5	65	510	0.13	32.5	32
7	6	42.5	510	0.08	21.25	21
8	7	0	510	0.00	0	0

Table 1: Grayscale value calculation

5. Resist development

Once exposed, the wafer needs to be developed using a developer. Note that for thick photoresist, such as SPR 220-7 which was used in this case, a hold time of at least 45 minutes is required between exposure and development to allow water vapor to diffuse into the resist and complete the reaction. Otherwise, bubbles may form during the post-bake and development step. We used the developer track ‘svgdev’ in SNF with the developer MF-26A. A 60 second post-exposure bake was done to improve resist adhesion, followed by development using recipe #6. No hard bake is required for SPR 220.

Characterization

Once photolithography is completed, samples need to be examined and characterized, primarily to compare the desired outcome and the actual outcome. This knowledge can then be used in process optimization and obtaining more accurate results. Characterization techniques can be simple and inexpensive while providing little detail (example: optical microscope), or complex and expensive while providing a high amount of detail (example: SEM). In our case, we used a variety of imaging and profilometry tools, which are described below:

1. Optical microscopy

The simplest and most inexpensive characterization tools available at SNF are a number of optical microscopes. Fig 9 shows an optical image of a 7 layered square with a 25 degree slope which was obtained immediately after developing. While the image has less detail than an SEM image, it still provides qualitative information (that grayscale lithography worked, since we see seven distinct layers) and some quantitative information (the slope is approximately what it should be, and the width of each layer is approximately correct).

Fig 9: Optical image of a corner of a 7 layered square

2. Confocal microscopy

To obtain quantitative information from an optical image, we made use of interferometry tools in SNF (the S-neox) and SNSF (the Keyence).

S-neox: The S-neox has a number of objectives (10x, 20x 50x, 150x) and two imaging modes, namely, interferometry and confocal mode. In interferometry mode, the user can choose the wavelength of incident light depending on the spectral reflectivity of the sample. Confocal microscopy, on the other hand, does not depend on the wavelength of light used which is why white light is used (to counter the possibility that spectral reflectivity of some samples might be really low at some wavelengths). The vertical resolution in both modes is very high (~10 nm), but the lateral resolution is limited to about half a micron.

Since our photoresist was not very reflective, we could not obtain accurate results unless we sputter coated the sample with metal. Fig 10 shows an image and the corresponding profile data from S-neox after sputter coating with 25 nm of Ti using the Lesker sputter coating tool. While the overall feature height is correct (~7 um), the steps cannot be seen clearly. It is not clear how much of this is due to the resolution limit of the Heidelberg (which is ~1 um), damage caused by sputter coating, and the lateral resolution limit of S-neox (which is ~0.5 um).

We switched to a gentler sputter coating process using the Hummer in Exfab (alternatively the Cressington coater in the SNSF can also be used), and analyzed images with the Keyence microscope. The samples were coated for ~ 20 minutes in Hummer. The thickness was not measured, but this would probably yield a film of around 10 - 15 nm thick.

Keyence: The Keyence is a confocal laser (408 nm violet light) scanning microscope that enables users to obtain high resolution (vertical ~1nm, horizontal ~ 0.12um) 3D profilometric images. Fig 11 shows an image from the Keyence with data, and it is seen that while the overall profile is fairly accurate, the steps aren’t exactly as designed. While this was not too critical for our application, a more detailed analysis of why there is a difference between the design and actual profile is warranted for the benefit of future users.

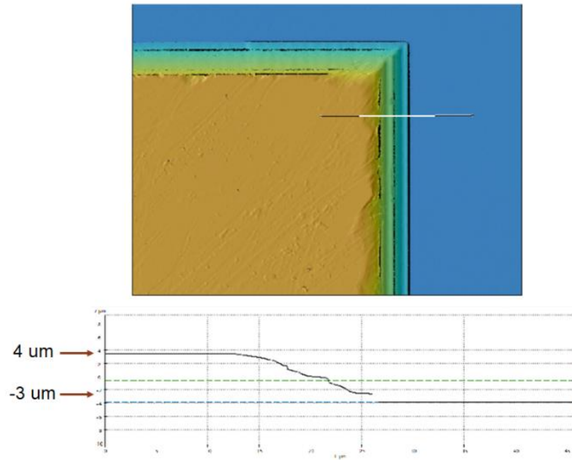

Fig 10: Image and profile data from S-neox

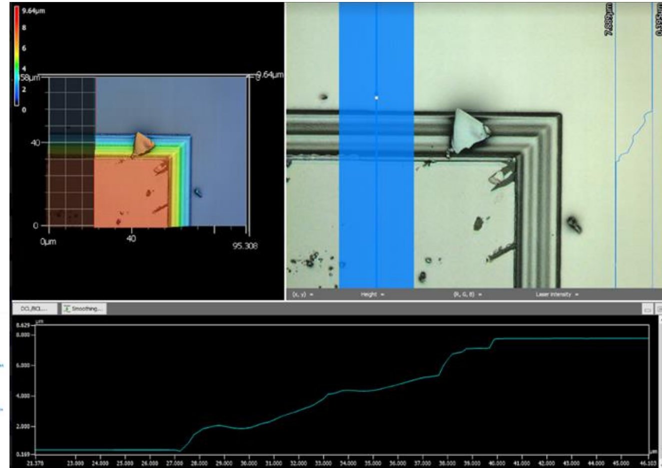

Fig 11: Image and data from the Keyence

3. Contact profilometry

Profilometry involves scanning a surface with a sharp probe and recording the motion of the probe. The resolution of a profilometer is of the order of the radius of curvature of the tip, and any features below this length will result in the tip imaging itself (or, the features playing the role of the sharp probe). We used the Dektak profilometer (resolution ~ 20 µm) in SNSF to measure resist profiles after reflow, and some of the results are shown in Fig 12 below.

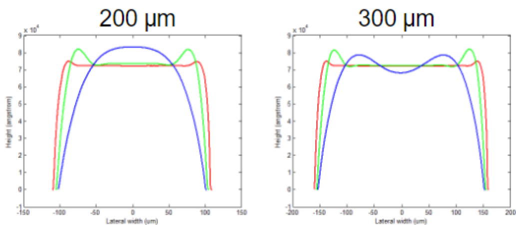

Fig 12: Dektak data from 200 um and 300 um resist samples after reflow at 120 C for 10 s, 2 min and 30 min.

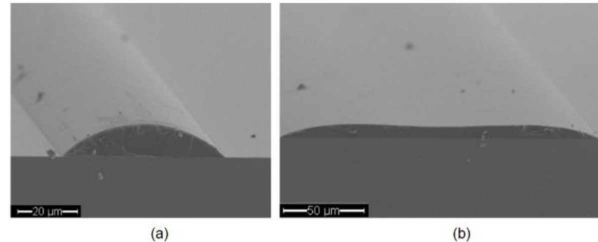

Fig 13: Cross sectional SEM image of (a) a 50 um feature and (b) a 200 um feature post baking at 120 C

4. SEM

Cross sectional SEM images of Hummer coated samples were obtained using SEM Sirion for select cases for the sake of clarity and comparison with data from the profilometer. A sample image is seen in Fig 13 above, showing final resist profile after baking a long rectangular feature at 120 C for 2 minutes. While we have yet to do an exact profile comparison between the measurements obtained from different tools, at first glance the images are consistent in the overall shapes that they describe, giving us some measure of confidence in our measurements.

II. Resist reflow studies

Introduction

While the thermal softening and reflow of developed photoresist structures is undesired for most applications as it degrades the patterned structure, it is well-suited to obtaining smooth, continuous profiles, complementing digital lithography, which is intended to give discrete levels. A natural application is in micro-optics, whereby reflow of photoresist can be used to transfer lens-shaped structures into the substrates by dry etching.[6] These microlenses could be used for collimation, illumination, and imaging in areas like optical fiber communications, computing, image processing, laser and detector arrays, etc. Another area of common use is in microfluidics, where channels are sometimes designed to have curved cross-sectional profiles to facilitate flow control using “push-up” or “push-down” valves.[7] ‘Wavy’ grating structures patterned in a herringbone formation have also been used to capture circulating tumor cells, as shown in Fig. 14c.[1] Additionally, it has been reported that electroplating onto photoresist microlens is a reliable method which allows the fabrication of high quality metallic molds for hot embossing.

Fig. 14a: Microlenses

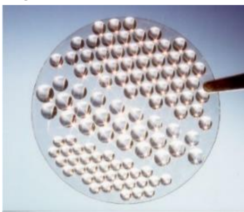

b: Microfluidic valves

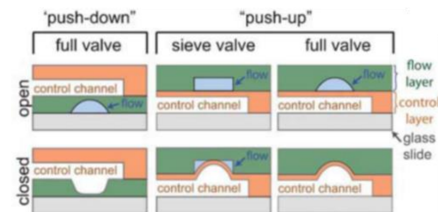

c: Microfluidic cell capture

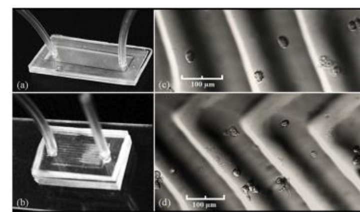

Resist reflow has the advantage of being very cheap to implement. However, the reflowed profile is often hard to predict, owing to its sensitivity to a range of factors. In this section, we set out to clarify some of these relationships through a set of splits on simple rectangular resist structures.

Our study complements others reported in the literature.[2-9] It:

- draws together the contribution of bake temperature, time and initial resist dimensions—parameters that have individually been found to affect reflowed features but have yet to be combined in a single model
- allows us to predict not just spherical / cylindrical “1-lobe” structures but also 2-lobe ones, identifying the ‘transition’ through a classification scheme
- uses a hybrid empirical-analytical model to simulate resist profiles in a way that does not require finite element calculations. From the inclusion of bake time as a split, we are also able to track resist evolution over time

Physics of Resist Reflow

Resist reflow can be a complex process involving a number of effects such as surface tension, edge stress, dilation/volume changes etc. During the melting procedure, the edges of the resist structure start melting above the softening temperature. Above the glass transition temperature,

the amorphous resist polymer changes abruptly from a rubbery state into a glassy state. The surface tension tries to minimize the surface area by rearranging the liquid masses inside the drop. In the ideal case, the resist melts completely, the masses are freely transported and surface tension forms a hemispherical shape. In practice, complete melting of the resist drop is not always achievable, especially not in the case of large and flat resist cylinders. For large resist volumes, the outer part of the liquid drop might already be crosslinked (due to outgassing of the solvents), before the inner part is completely melted. The goal of this section is to give an overview of these effects, and to provide a foundation for further investigation.

Surface tension

Surface tension tends to minimize interfacial area so as to minimize energy. Therefore, a blob of Newtonian liquid on a surface, when baked, tends to become spherical in shape (Fig. 15a).

The final shape must satisfy two constraints: (1) the contact angle is predetermined by the surface tension between the resist and air, between resist and the substrate and that between air and the substrate, and (2) the final volume must be equal to the initial volume, for the case where there is no volume change, or it must be some fraction of the initial volume when there is volume change.

In the case of resist reflow, it is important to note that a resist shows visco-elastic behavior and does not behave like a Newtonian liquid. For example, the contact angle is highly dependent on bake conditions because local molecular structure and interaction changes with temperature. While this can make analysis and modeling complicated, the general principle of surface and energy minimization still remains true, albeit locally.

Edge Stress

A resist structure is subjected to various processes during fabrication, such as spin coating, exposure, development etc. These processes can leave the edges of a resist under a state of stress as shown in Fig. 15b (top). When the feature is heated, it relaxes and this can result in curvature and the formation of lobes as shown in Fig. 15b (bottom).

Fig. 15a:

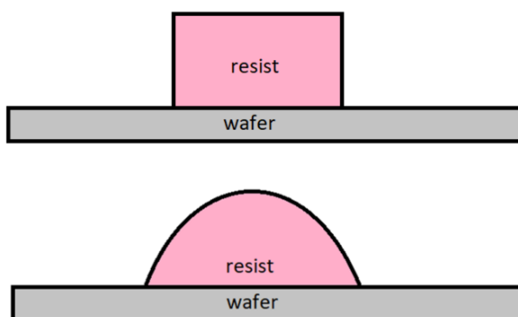

15b:

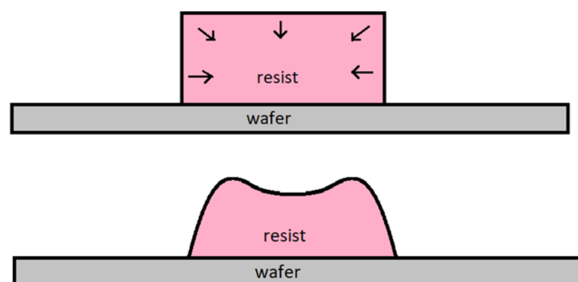

Volume Changes

Volume changes of photoresist may or may not occur depending on the resist and process conditions. Our experiments show that features made from SPR 220-7 undergo volume reduction of up to 15% depending on feature size and bake conditions. For example, Fig 16 shows normalized final volume when features of different sizes are baked for different times at 180 C.

Fig. 16: Variation of normalized resist area with vertical aspect ratio and $\log_{10}$(bake time) for reflow at 180 C

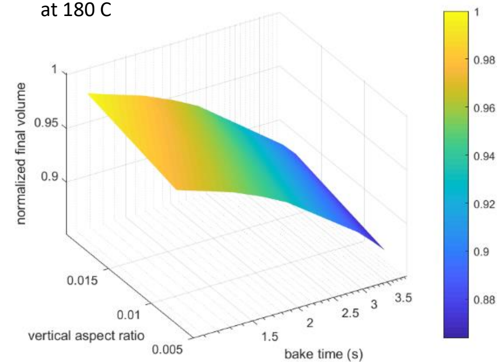

Experimental objectives & methodology

We chose to focus our reflow experiments on characterizing the dependence of reflowed resist shape on these independent variables: (1) bake temperature, 2) bake time, 3) resist width, and 4) lateral aspect ratio. The splits chosen are shown in the figure below. Lateral aspect ratio was investigated with two splits: resist patterned with a square shape (i.e. length = width), and resist patterned as a long strip (length = 4.75 mm). The former would ostensibly behave more similarly to the circular resist patterns used to create microlenses, while the latter would be a more useful comparison for the rounded channels used in microfluidics. Further background on why these input variables were chosen is covered in the report accompanying this project.

Resist test structures were fabricated by patterning 7μm resist using Heidelberg, and reflowing on a hotplate. The resist profiles were characterized by profilometry, using Dektak – this was chosen due to its ease of use and of exporting the data in easily analyzable CSV format. The main drawback of this method is that it was difficult to standardize the exact cross-section measured and ensure that the profiler was traversing perpendicular to the edge; as such, the widths obtained may not be accurate.

The Dektak data was processed in Matlab in the following sequence:

i) The raw data was leveled
ii) The left and right edges of the resist structure were identified from peaks in the 1st derivative of the profile data
iii) Specific dependent variables were extracted from the profile, namely
    a. Height of the resist structure at its midpoint
    b. Number of resist lobes (1 central lobe or 2 side lobes)
    c. Average side lobe height (if applicable)
    d. Average side lobe position, defined from the edge of the resist structure (if applicable)
    e. Contact angle at the base of the resist structure
    f. Cross sectional area, taken as a proxy for resist volume (obtained by integrating heights across the width of the resist)
iv) The profile data was aggregated alongside the sample names and independent (X) variables in a structure, while the extracted dependent (Y) variables were appended alongside the

independent variables in a summary table. These were used to model resist behavior, as will be described next.

The extracted dependent variables were chosen to collectively offer a reasonable reductive description of the overall shape of the resist. Fig. 17 shows a summary of the independent variables chosen for the splits and the dependent variables measured from the data.

Fig. 17: Summary of independent and dependent variables in resist reflow experiment

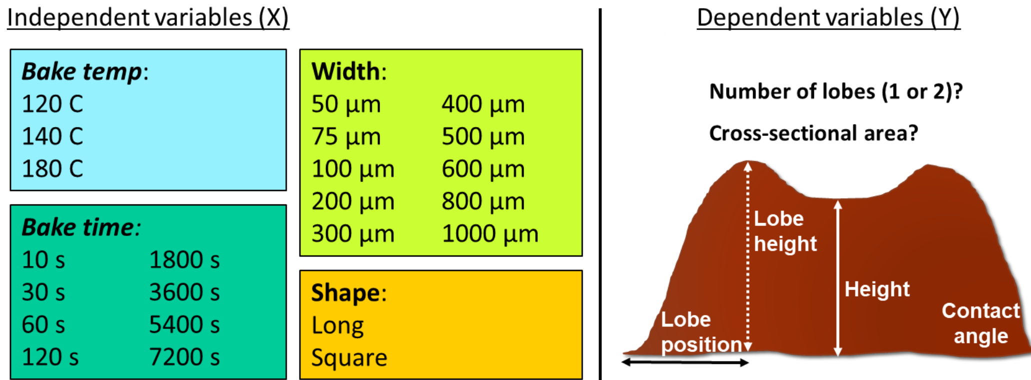

Analysis strategy

Having obtained the raw profile data and extracted relevant resist features from it, we began analyzing trends by first visualizing relationships between the dependent and independent variables via scatter plots. These can be found in the Results subsection and Appendix.

Two main things were observed: first, we found that the dependent variables (height, lobe height, lobe position, contact angle) seemed to vary roughly linearly with the independent variables (bake temperature, $\log_{10}$(bake time), vertical aspect ratio, shape). Vertical aspect ratio is obtained by dividing the resist height (~ 7 um) by width, and was used to allow for the model to possibly be used with other resist heights in the future. Shape was taken as a binary variable, taking a value of 1 if the resist was square in shape, and 0 if the resist was long. In view of this, we chose linear regression as the first model to fit to the data. The aim is to obtain empirical relationships from which the resist dependent parameters can be predicted given an arbitrary set of input variables.

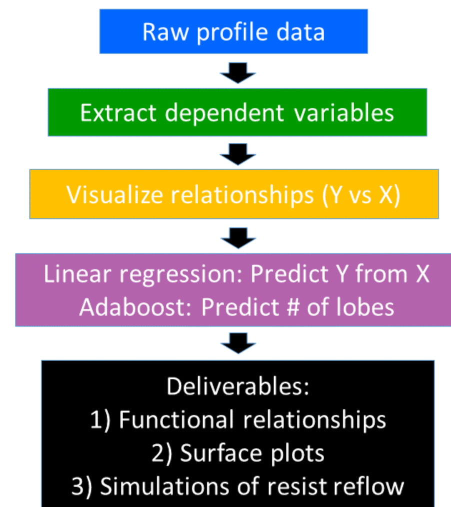

The second observation was that the derived variables seemed to follow different trends when the resist had 1 lobe versus 2 lobes. 'Small' resist structure (< 100 µm) trends also seemed to be described by different linear coefficients compared to 'large' resist structures (100 – 1000 µm). As such, we chose to segment the data into 4 groups: 1) 2 lobes, large; 2) 1 lobe, large; 3) 2 lobes, small; 4) 1 lobe, small, and to run separate regressions on each set of data.

In order to decide which regression fit to use to predict the shape of reflowed resist, we would thus need classify a sample according to whether it has 1 or 2 lobes after the reflow process. Fig. 18 shows a visualization of all our data of sample size N = 482, plotted against vertical aspect ratio and bake time, labeled according to the number of lobes. As can be seen, the boundary between the two classes is rather straightforward, which suggests that a simple machine learning model should be able to predict it. To do this, we first tried a logistic regression model, with the result shown in Appendix 1. This resulted in a prediction error of ~ 10%— passable but not great. We then tried an ensemble learning method called Adaboost (available as a function online). The model obtained from training on all our data gave a prediction error of ~ 2.95%. This seemed reasonable for the small sample size and was thus adopted for the classification scheme.

Fig 18. Visualization of # of lobes in reflowed resist structure as a function of input variables

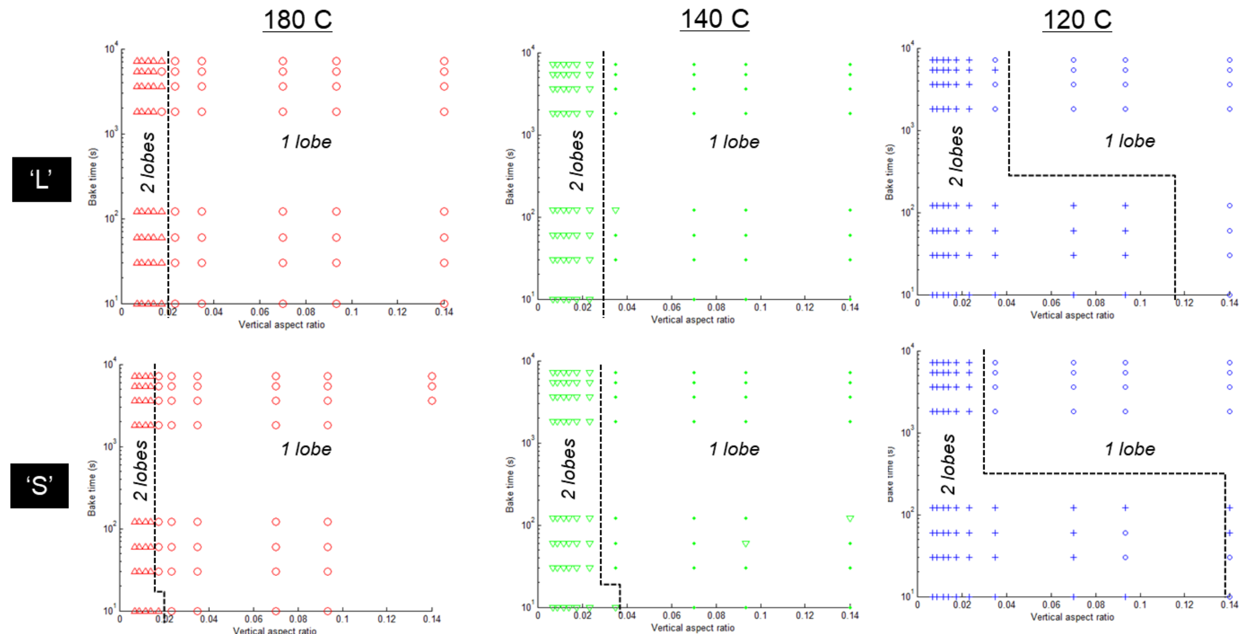

The functional regression relationships obtained allow us to plot 3D surface plots, which succinctly describe the variation of resist properties (i.e., dependent variables) with input parameters and reflow history (i.e., independent variables). From these dependent variables, we are also able to reconstruct a smooth resist profile and trace the evolution of resist with various bake times. A summary of our data analysis procedure is laid out in the flowchart above.

Results

Resist profile data

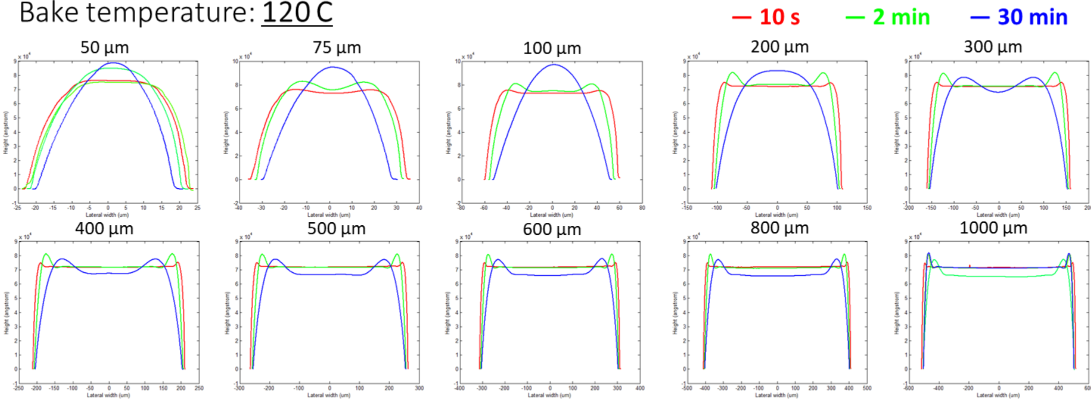

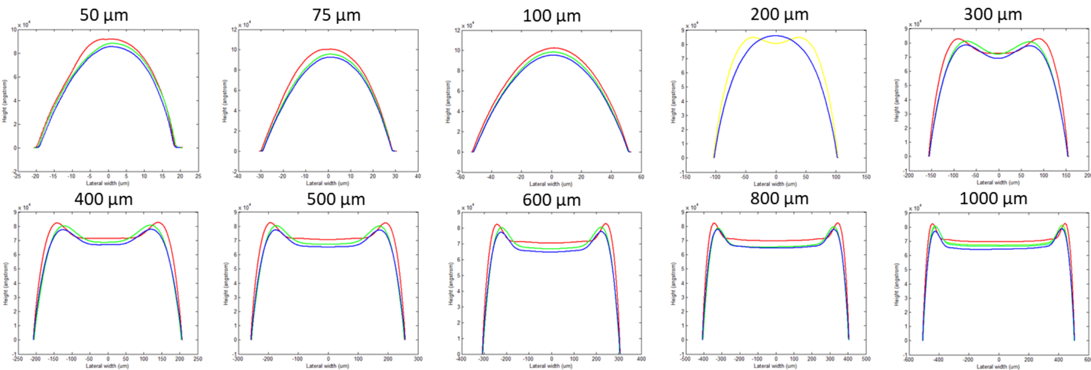

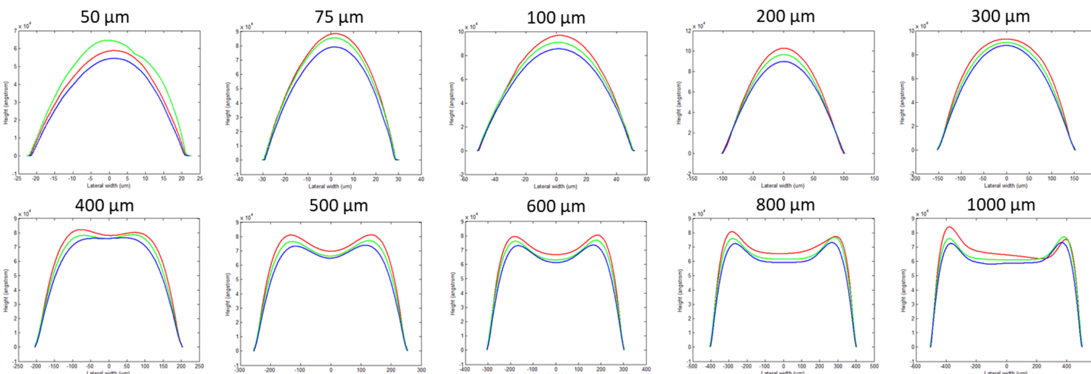

Although the data we obtained across 480 splits was diverse, some general comments about trends can be made:

- Resist profiles show increased curvature and decreased contact angle with an increase in bake time or bake temperature. Contact angle is fairly independent of feature size, suggesting local effects are dominant.

- Volume seems to decrease with bake time, and bake temperature seems to play a minor role. Smaller features tend to exhibit a larger fractional volume change of about 15 - 20 % as compared to larger features.
- Whether a feature ends up with a single bulge or two lobes at the edges depends largely on the aspect ratio, and to some extent on the bake time/temperature. Larger features (height/width<0.35) tend to form structures with two lobes, irrespective of bake temperature and time, while smaller features form both one and two lobed structures, depending on bake time and bake temperature.

Linear regression & Surface plots

Linear regressions were run in MATLAB for the following dependent variables → normalized final area/volume, contact angle, center height, lobe height offset, lobe position, as functions of four input parameters → feature size (represented as the ratio of pre-bake resist height to width, or vertical aspect ratio), bake time, bake temperature, feature shape. An example is shown for contact angle data, plotted along the dimension of bake temperature in Fig. 20. We obtained empirical linear equations that enables users to calculate the five dependent variables and construct an approximate final resist profile based on process and initial conditions. In this example, the fit to the data was: $\boldsymbol{y = 64.87 - 0.00176 * x_1 - 0.29 * x_2 - 2.8015 * x_3}$, where y: Contact Angle, x_1: vertical aspect ratio, x_2: bake temperature & x_3: $\log_{10}$(bake time). A summary of coefficients obtained from the fits is provided in Appendix 2. 3D surface plots of the dependent variables against bake time and vertical aspect ratio at each bake temperature all for four data segments are presented in Appendix 3, allowing us to visualize trends in the data fits.

Fig 20: Scatter plot of for contact angle data plotted against bake temperature

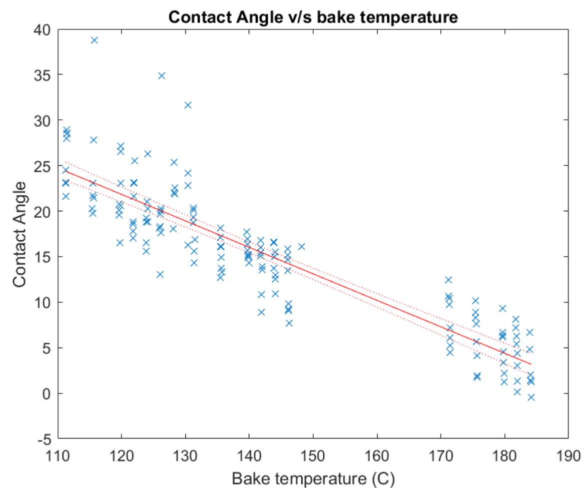

Use case & Simulations

Given values of input variables (resist dimensions, bake temperature), we are thus able to predict dependent features of the reflowed resist.

i) **Predict the number of lobes** resulting from the reflow process. This would tell us which of the 4 data segments it belongs to, and hence which regression fit to use.

If the *adaboost* function is used in Matlab and a *model* has already been trained, the prediction can be done simply by creating a vector of the dependent variables
i.e. `Xvar = [1; log10(baketime); baketemp; aspectratio_vert; shape_int]`
and running: `estimateclass = adaboost('apply',Xvar,model);`
whereby a result of -1 corresponds to 1 lobe, and +1 to 2 lobes.

ii) **Predict Y parameters** that describe the resist height, lobe height, lobe position, contact angle and number of lobes from the regression fit.

Additionally, we built a tool that would simulate the shape of the resist after a given bake time. Starting off from the predicted the Y parameters, we then:

iii) Reconstruct the left half of the resist profile using a set of 1 (for 1 lobe structures) to 3 (for 2 lobe structures) cubic splines. We assume the right half of the profile is a mirror image of the left. The cubic polynomial equations would satisfy conditions determined by the predicted Y parameters. This can be formulated into a set of 4 simultaneous equations for each cubic spline. Solving these produces 4 coefficients which would define the spline: $y = \beta_0 + \beta_1 x + \beta_2 x^2 + \beta_3 x^3$).

iv) Calculate resist height (Z) values at specific sparse points along each spline using the fitted coefficients. When joined together, this gives a rough ('jagged') outline of the reconstructed profile.

v) A second cubic spline interpolation is applied to this sparse set of Z values using the inbuilt function *csaps*. This results in a continuous profile (Z_{smooth}) and 1st derivative of the profile.

vi) Predict normalized resist cross-sectional area using the appropriate regression fit. Scale Z_{smooth} to get the same cross sectional area as predicted.

vii) Plot the result—this is the simulated profile.

Using this procedure, we were able to get realistic looking resist profile simulations which were not far off from the measurements. An example for 300 um wide 'long' resist structures is shown in Fig. 21. Nonetheless, there remains much room for improving the accuracy of our predicted structures. Steps that would help include:

- Incorporating more training data and repetitions
- Extracting more Y variable features from the profile data to describe the resist shape
- Using a more refined machine learning model than simple linear regression
- Improving the spline interpolation method used to reconstruct the resist profile

Fig. 21a: Reflow at 120 C from 10 s → 2 h

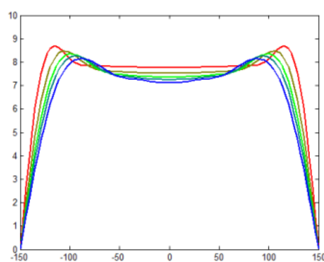

21b: Reflow at 140 C from 10 s → 2 h

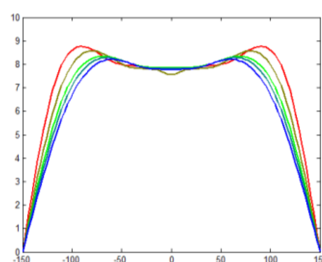

21b: Reflow at 180 C from 10 s → 2 h

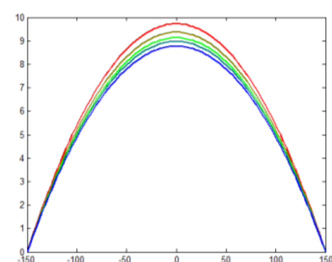

III. Parylene pseudo liftoff process

Introduction

Parylene is an exceptionally robust polymer that can be deposited in thin conformal films, making it a great option for moisture resistant biocompatible device encapsulation. The main method of patterning parylene uses oxygen plasma. However, this may not always be compatible with other materials in the device (e.g. underlying organic films), and may leave residue in the active site.

With this in mind, we seek to develop an alternative, ‘pseudo lift-off’ process for patterning parylene. As shown below, the idea is to pattern resist (layer 1) in the inverse of the pattern that would typically be etched out in the parylene, to deposit parylene over the whole structure, and then perform a second lithography step (layer 2) which would allow the parylene coating the first layer of resist to be removed. Finally, the layer 1 of resist and the remaining layer 2 of can be dissolved with a solvent (a gentler process than O_2 plasma), leaving the patterned parylene. It would be advantageous for the layer 1 resist to have sloping sidewalls, so that the parylene coating the walls can also be removed without leaving ‘dog-ears’.

Fig. 22: Process flow for parylene pseudo-liftoff process

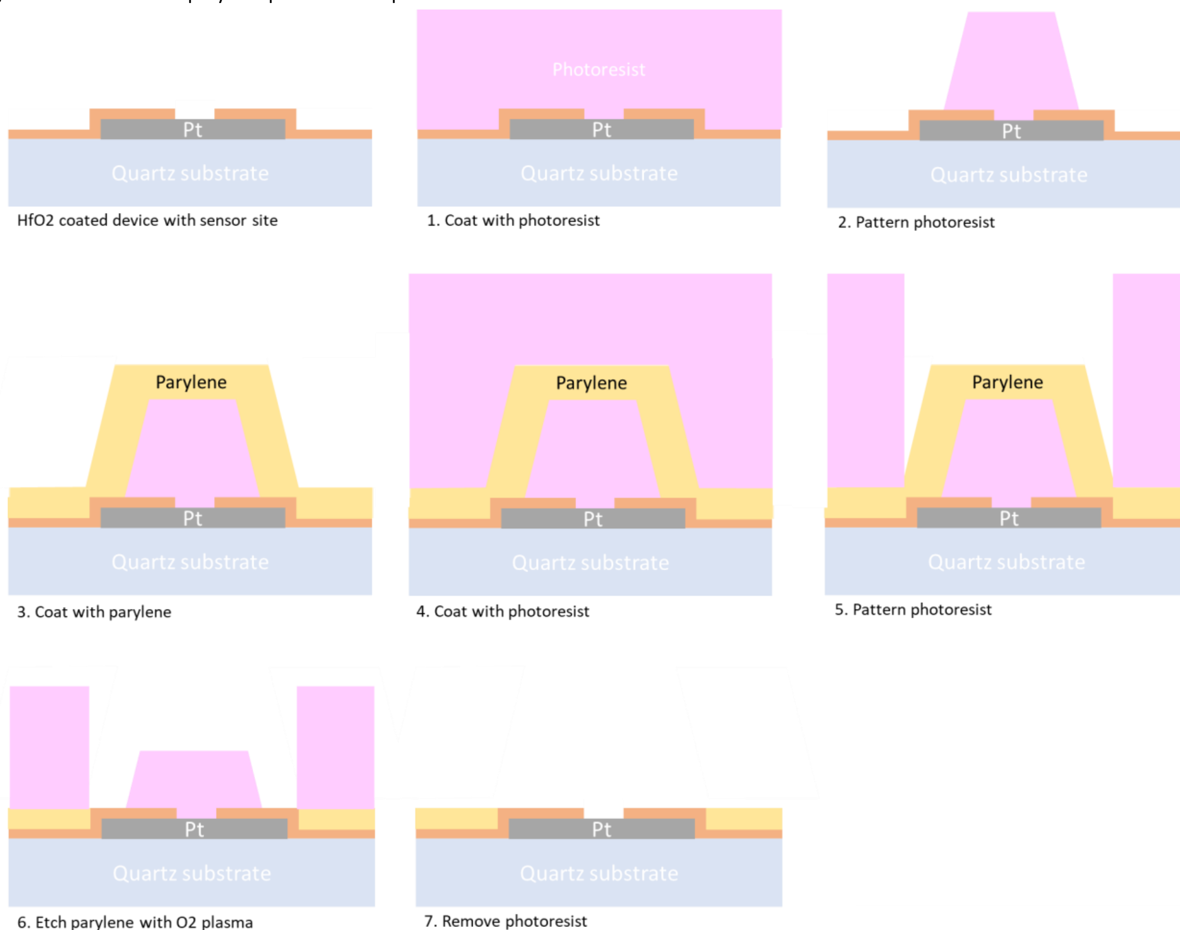

Process development

Achieving tapered sidewalls in 1st layer of photoresist

To develop this process, we explored 3 different ways of achieving sloped sidewalls on resist: 1) grayscale lithography, 2) brief immersion in isopropanol (IPA) to preferably remove the sharp corners of resist, and 3) resist reflow by baking on a hotplate. 7 um of SPR 220 resist was spun onto a silicon wafer and a 8x8 array, each containing squares of side 1000, 500, 100 um, was patterned using Heidelberg (dose 510 mJ/cm2, defocus -2). Unfortunately, due to the need to take the wafers out of the Litho area after development for dicing, the resist ended up exposed and was quickly dissolved completely by the IPA upon immersion, preventing us from fulling testing the IPA method.

7 and 14 layer grayscale lithography were attempted with success (but without fine-tuning precise layer thickness / doses), giving a discretely stepped sidewall as seen in images in the previous section. Some of these grayscale samples were baked on hotplate for 2 minutes at 120 C—the resultant profile showed a smooth curved profile, with no remaining trace of the grayscale steps. By performing a control bake on resist that had not been patterned with grayscale (i.e. with vertical sidewall), it was found that the post-reflow shape of the resist was pretty much independent of whether it had been process with grayscale or not. As the post-reflow profiles offered a more gradual and smoother sidewall taper, we chose to focus on this method. A more extensive characterization of photoresist reflow is described in the subsequent section of this report.

	Pros	Cons
Grayscale lithography	More precise control of sidewall profile	More time consuming Discrete sidewall steps formed
Resist reflow	Simple, cheap	Need for careful control of bake parameters (time, temperature) to achieve precise shape – but this may not be that important for this application

Parylene deposition

Parylene deposition was done using the parylene coater in Exfab room 155. 1 µm of parylene was deposited using 2 µg of parylene dimer, in a process lasting ~4 hours (including cool down time). Note that as the process is highly conformal, the backside of samples does get coated as well—which could pose sample compatibility issues with downstream tools, for example Pt-Ox, in which edge polymer could result in the wafer getting stuck to the clamp. To avoid this, we covered the backside of our wafers with blue tape from the dicing area, which could be easily removed after parylene deposition to leave a clean backside.

Patterning photoresist layer 2 & O_2 plasma etch

The 2nd photoresist layer was patterned in the inverse of the pattern in layer 1. Its function is to cover the areas where we want the parylene to remain, and to expose the parylene covering the 1st layer of photoresist (which is to eventually be lifted off) to the subsequent O_2 plasma etch.

Pt-Ox was chosen to perform the O_2 plasma etch, mainly due to its compatibility with all cleanliness levels, and the availability of characterized recipes. [Important: to prevent wafers from getting stuck in the tool it is important to perform edge bead removal for all resist layers spun, and furthermore remove resist from the flat using a q-tip. Furthermore, parylene coating the exposed edges needs to be scraped away using a blade.] Using the recipe “charmaine_parylene-etch”, parylene with an initial thickness of 1050 Angstrom is expected to be completely etched within 80 s, as illustrated in Fig. 23. Allowing for an over-etch of 120%, we first chose an etch time of 3 minutes. Surprisingly, a significant amount of parylene was left over after this etch, mainly at the boundaries of the resist structure from layer 1 (see Fig. 24). It is possible that the resist there is slightly thicker there owing to the way the parylene drapes over the resist structure underneath, or that etch rate at the boundaries is lower due to the fact that the parylene there is suspended and not in contact with the underlying substrate.

Fig. 23: Parylene thickness vs etch time

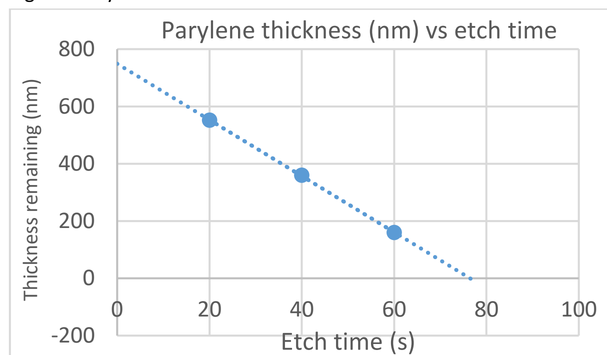

Fig. 24: Optical image from iteration 1 of parylene liftoff process development (after 3 min O_2 etch → resist removal)

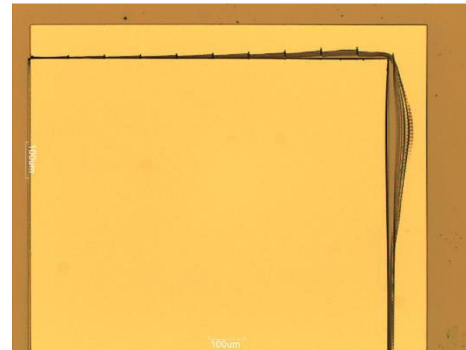

We went through 3 iterations of these steps to optimize the etch process to leave minimal parylene residue, using the following pairs of conditions:

i) 7 µm of PR (layer 1) → reflow @ 120 for 2 min → 1 µm parylene deposition → 3 µm PR (layer 2) → 3 minutes O_2 etch
ii) 7 µm of PR (layer 1) → reflow @ 120 for 2 min → 1 µm parylene deposition → 7 µm of PR (layer 2) → 6 minutes O_2 etch
iii) 7 µm of PR (layer 1) → reflow @ 180 for 2 min → 1 µm parylene deposition → 10 µm of PR (layer 2) → 10 minutes O_2 etch

Images taken from process (iii) are shown in Fig. 25 below. The amount of residue left after the 10 minute etch employed here is barely visible from the optical images, but can still be seen in the SEM images (see next page). To try to get rid of the residue, a further 5 minute descum was done on Drytek2 post Pt-Ox etch, using 500W power, 150 mTorr pressure and 100 sccm O_2.

Fig. 25: Different stages of process in iteration 3

Pre PR development	Post PR development	Post O2 etch	Post resist removal
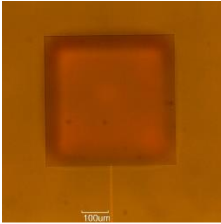	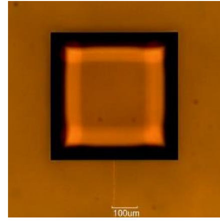	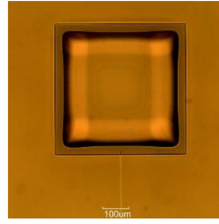	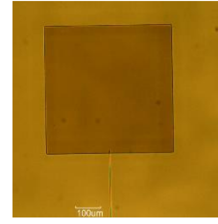

SEM imaging results

Fig. 26: Post-process SEM results

a) After 6 min O2 etch ➔ resist removal

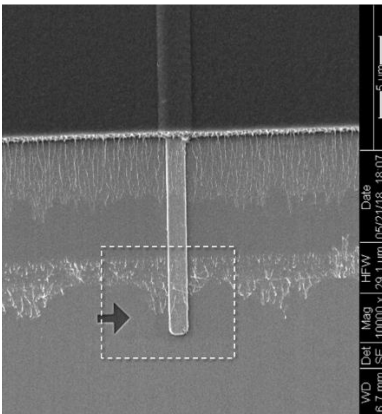

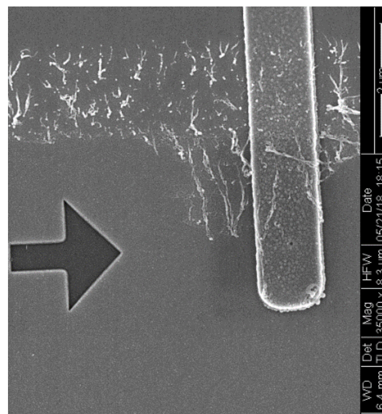

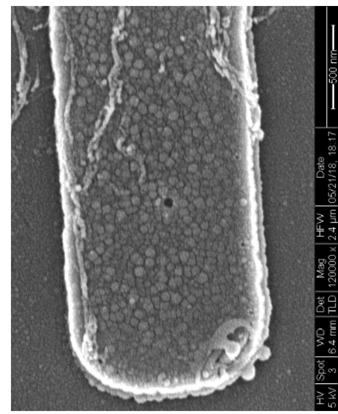

b) 6 min O2 etch ➔ resist removal ➔ 5 min descum

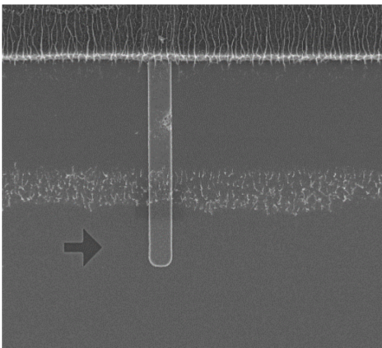

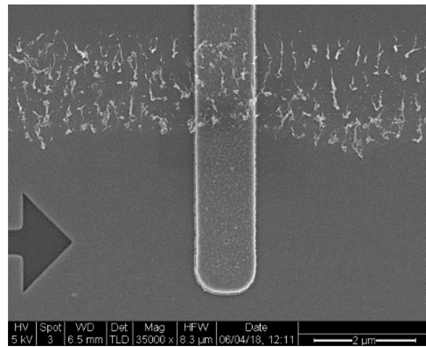

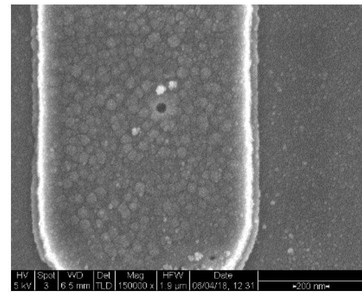

c) 10 min O2 etch ➔ resist removal

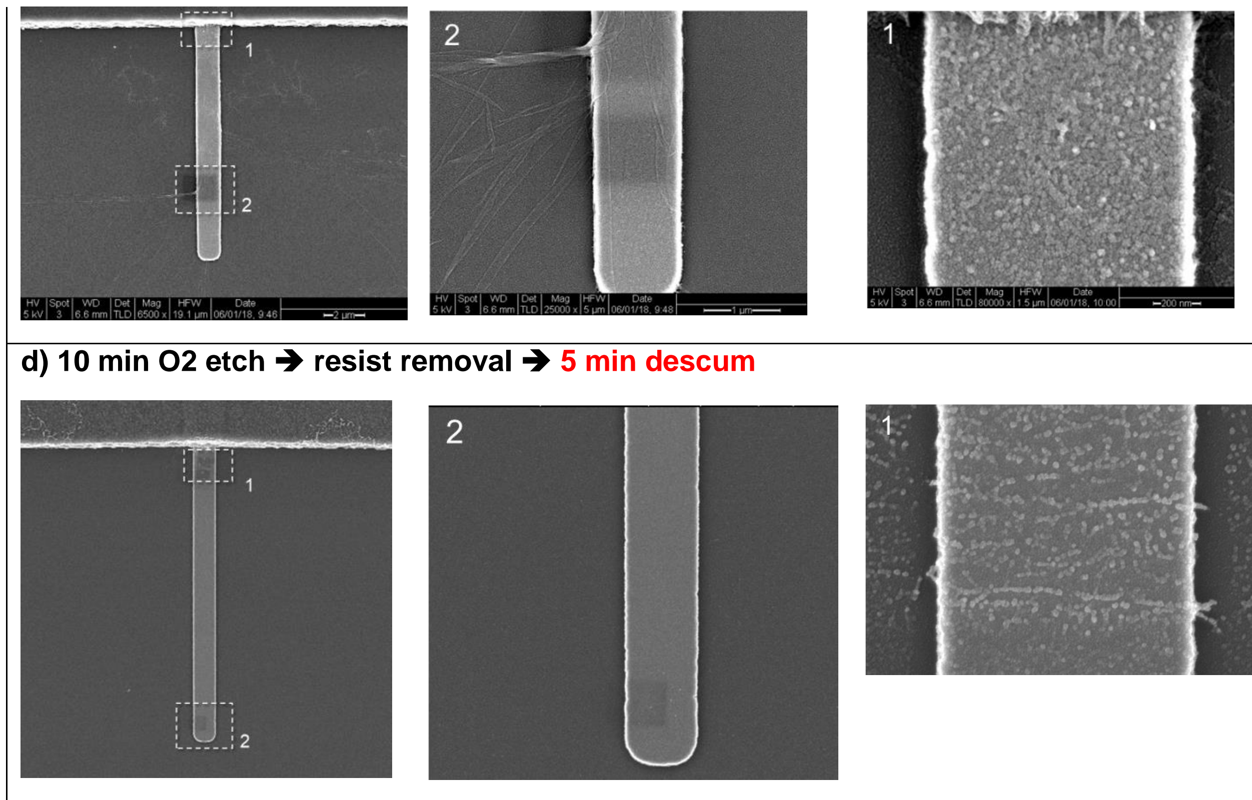

In the Fig. 26 above, row (a) depicts a device exposed from the area where parylene was removed via a 6 minute O_2 etch. Row (b) shows a similar device, after the additional 5 minute O_2 descum. Row (c) shows a device post 10 minute O_2 etch, and row (d) shows the result after a 5 minute O_2 descum.

Several features are noteworthy. First is the filamentary form of the parylene residue in row (a) compared to the thin gauze-like form in (c). It's not clear why residue looks different, but it may have something to do with the thickness of the residue and the specific topography of the parylene atop the reflowed resist, especially at the edges. The 5 minute O_2 descum seems to reduce the extent of the filamentary residue (row b) slightly, while significantly reducing the visibility of the thin sheet-like residue (row d). Some boundaries of the sheet-like residue are nonetheless remain, and appear as small blob-like scales, as seen in the close-up labelled 1.

Further iterations are needed to fully optimize this process. We would recommend a slightly longer etch (perhaps around 12 minutes) to fully remove the residue, which would in turn necessitate a 10 um thick photoresist for layer 2. Note that the longer etch period would also mean that more resist from layer gets eroded at the edges of the pattern. So in order to protect sensitive areas, from exposure to O_2 plasma, the layer 1 pattern area may need to be scaled up accordingly.

Parylene patterning using aluminum as the pseudo-liftoff layer

Given the drawbacks of using thick reflowed photoresist as the liftoff layer, we explored using a metal as an alternative material to mask the area where the parylene is to be removed. A metal masking layer would offer much higher selectivity against the O_2 plasma etch of the parylene compared to photoresist, giving better pattern fidelity as its edges would not be eroded. As such, we would also be able to get away with a thinner masking layer, meaning that the 'dog-eared' parylene residue left at its edges after the pseudo-liftoff stage would be less prominent, and may not even be an issue. The downside would be the need for additional deposition and removal steps of the metal masking layer. However, it turned out that the removal of masking layer via a wet etch facilitated getting rid of the parylene residue that remained an issue even with the extended etches introduced with the photoresist masking method.

Furthermore, it was found that adhesion of parylene to the substrate could be improved by priming with the silane A-174 (available in the Exfab). The standard HMDS priming used before spin-coating photoresist gave poor adhesion – in fact, the parylene peeled off during the dicing process. Not doing any surface treatment prior to parylene deposition gave better adhesion than HMDS; nevertheless, upon immersion of a sample into a SC1 solution (5:1:1 ratio of DI water, 30% H_2O_2, and NH_4OH) at 70 °C for 45 seconds, the parylene started delaminating slightly at the edges of the sample.

Finally, we found that in order for the edges of the Al mask pattern (defined by photoresist layer 1) and the edges of the pattern defined by photoresist layer 2 to coincide, it was necessary to decrease offset the positions of the edges of photoresist layer 2 by around 5 µm. For example, in order to pattern a square well in the parylene of 1000 x 1000 µm, the square well defined in photoresist layer 2 would need to be ~ 995 x 995 µm.

The latest process flow developed for this technique is summarized below:

1. *Photoresist layer 1*: Spin 1.6 µm of 3612 resist
2. Pattern photoresist with Heidelberg, with resist exposed and removed where parylene is to be removed.
3. Deposit *80 nm of aluminum (unspiked by Si) with Lesker.
   *Note: If there are devices underneath the metal masking layer, ensure that the thickness of the aluminum exceeds the device thickness so that the sidewalls are covered.
4. Aluminum liftoff in acetone, followed by sonication in PG remover for 5 minutes, IPA rinse and blow dry. This will leave the Al masking layer remaining in regions where we do not want parylene deposited on the substrate.
5. Deposit parylene adhesion layer, A-174 silane by immersion.
   - Prepare a mixture of DI water, IPA, and A-174 silane in the volume ratio of 100:100:1.
   - Stir the mixture for 30 seconds and allow to stand for at least 2 h to react. The solution can be kept for up to 24 h.
   - Immerse sample in mixture for 15 – 30 minutes.
   - Remove sample and allow it to air dry for 15 – 30 minutes.
   - Rinse sample in IPA for 30 seconds. Blow dry.
6. Cover backside of wafer with blue dicing tape.
7. Deposit 2 µm of parylene.

8. *Photoresist layer 2*: Spin 10 µm of SPR 220-7 resist with 2 mm edge bead removal.
9. Pattern with Heidelberg, with resist removed where parylene is to be removed. However, the pattern size is shrunk by 5.2 um compared to the pattern used in step 2. The size offset is necessary to ensure the edge of the sputtered Al and edge of the patterned parylene coincide. (Note: a 3 h hold is needed before development, to ensure that the reaction of the exposed resist is complete.)
10. Use a q-tip to remove resist from the flat of the wafer (if the sample is a wafer). Then use a blade to scrape the parylene film off the perimeter of the wafer.
11. O2 plasma etch exposed parylene for 10 mins in Pt-Ox.
12. Remove photoresist layer 2 by rinsing in acetone and IPA. Blow dry.
13. Remove Al masking layer by immersing face down in Al etch A for 10 min. Rinse in DI water and blow dry.

Fig. 27a: Test sample with 1.5 µm thick parylene on Si. Edge of parylene pattern, after O_2 etch and Al removal

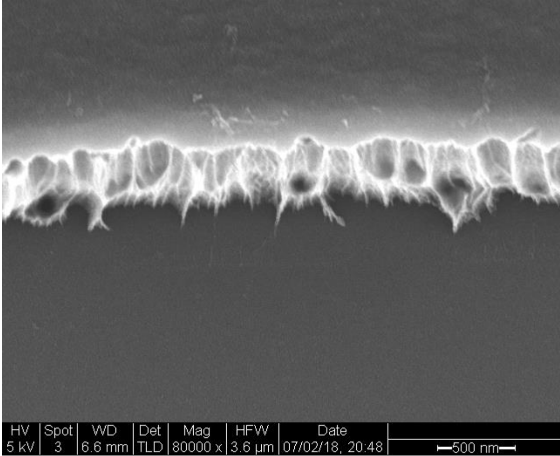

b: Pattern edge whereby parylene and Al mask edges are laterally misaligned by ~ 1µm

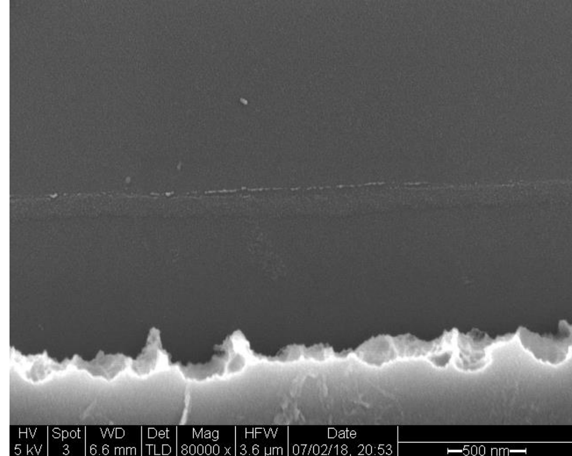

Concluding remarks

Summary

This project was started with the goal of developing a recipe for quasi-liftoff of parylene, with applications to biomedical device design in mind. The need to develop a process without leaving behind ‘dog-ears’ around the etched area led to the use of grayscale lithography and resist reflow to create inclined resist features. We found that that resist reflow worked well enough to produce inclined features, and was less time consuming than grayscale lithography on the Heidelberg. However, there wasn’t a reliable way to predict final profiles of resist after reflow, which is why a detailed study on the reflow of SPR 220 was carried out. Using the knowledge derived from resist reflow, a recipe for quasi-liftoff of parylene was developed.

Grayscale lithography

Grayscale lithography using SPR 220-7 was characterized using the Heidelberg, and the contrast curves have been made available for future users. A variety of characterization methods were used to study resist profiles after grayscale lithography and reflow, such as optical microscopy, interferometry, profilometry and SEM imaging. These methods have been compared and various pros and cons have been listed in this report.

Resist reflow

Resist reflow was studied for a variety of process conditions, and data consolidated. The physics of resist reflow was briefly touched upon in this report, and a number of physical mechanisms at play were listed. Using linear regressions on the data, empirical relations and surface plots were generated and have been made available for the benefit of future users. The raw data collected using profilometry for a large variety of process conditions has also been made available so that interested users can carry out their own analysis on the data.

Quasi-liftoff of parylene

A recipe for quasi-liftoff of parylene, employing 7 µm thick photoresist as the masking / liftoff layer, was developed and characterized. A number of issues with the process were highlighted, for example, residual parylene remaining after plasma etching and descumming. Aluminum metal was explored as an alternative masking material, which much better results.

Acknowledgements

We would like to thank the staff at SNF and SNSF, external mentors, and Prof. Roger Howe and Dr. Mary Tang for their support and invaluable advice throughout the course of this project.

References

1. He R et al. Generation of customizable microwavy pattern through grayscale direct image lithography. Scientific Reports. 2016; 6:21621.
2. Nussbaum P et al. Design, fabrication and testing of microlens arrays for sensors and microsystems. Pure Appl. Opt. 1997; 6:617.
3. O'Neill F et al. Photoresist reflow method of microlens production. Part I: Background and experiments. Optik 2002; 113(9):391.
4. O'Neill F et al. Photoresist reflow method of microlens production. Part II: Analytic models. Optik 2002; 113(9):405
5. Ashraf M et al. Geometrical characterization techniques for microlens made by thermal reflow of photoresist cylinder. Optics & Lasers in Eng. 2008; 46:711.
6. Roy E et al. Microlens array fabrication by enhanced thermal reflow process: Towards efficient collection of fluorescence light from microarrays. Microelectronic Engineering 2009; 86:2255.
7. Fordyce PM et al. Systematic characterization of feature dimensions and closing pressures for microfluidic valves produced via photoresist reflow. Lab on a Chip 2012; 12:4287.
8. Kirchner R et al. Energy-based thermal reflow simulation for 3D polymer shape prediction using Surface Evolver. J. Micromech. Microeng. 2014; 24:055010.
9. Liu H et al. Control of edge bulge evolution during photoresist reflow and its application to diamond microlens fabrication. J. Vac. Sci. Technol. B 2016; 34(2): 021602

APPENDIX

1. Classification of number of lobes

Logistic regression

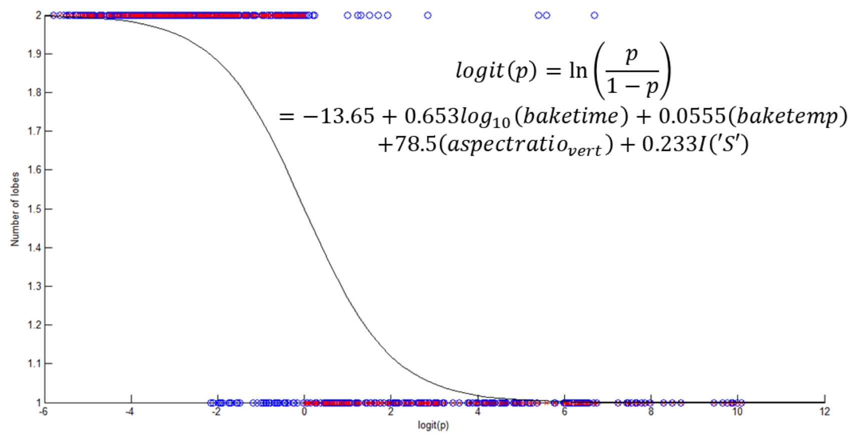

Adaboost

Model obtained after training on our data → this is input into the function to for inference on new samples.

alpha	dimension	threshold	direction	boundary	error
1.025635	3	0.023334	-1	[1,120,0.007,0,3.85733249643127,180,0.14,1]	0.113924
0.689435	2	140.0002	-1	[1,120,0.007,0,3.85733249643127,180,0.14,1]	0.113924
0.586054	3	0.014	-1	[1,120,0.007,0,3.85733249643127,180,0.14,1]	0.075949
0.450725	3	0.093333	-1	[1,120,0.007,0,3.85733249643127,180,0.14,1]	0.113924
0.414522	1	2.079191	-1	[1,120,0.007,0,3.85733249643127,180,0.14,1]	0.088608
0.383252	3	0.0175	-1	[1,120,0.007,0,3.85733249643127,180,0.14,1]	0.097046
0.466073	2	120.0003	-1	[1,120,0.007,0,3.85733249643127,180,0.14,1]	0.029536
0.269902	4	-1.00E-10	1	[1,120,0.007,0,3.85733249643127,180,0.14,1]	0.046414
0.293736	3	0.014	-1	[1,120,0.007,0,3.85733249643127,180,0.14,1]	0.029536
0.311412	2	140.0002	-1	[1,120,0.007,0,3.85733249643127,180,0.14,1]	0.029536

2. Linear regression coefficients

The data gathered has been segmented into 4 categories based on how consistent/uniform trends were in each category:

Category 1: Large structures (>100 um) with 2 lobes

Category 2: Large structures (>100 um) with 1 lobe

Category 3: Small structures (>100 um) with 2 lobes

Category 4: Small structures (>100 um) with 1 lobe

The following tables provide data for coefficients of the regression equations that we derived. Coefficients are listed for the five final parameters (area, height, lobe height offset, lobe position, contact angle) as per categories described above. The input variables are bake time, bake temperature, vertical aspect ratio, and shape integer (which is 1 for square and 0 for long rectangle).

Example: Looking at the table normalized area below, one could construct the regression equation for normalized area for large 2 lobed squares (category 1, shape integer 1) as follows:

Normalized area (um) = 8.5 - 0.27*log(***bake time***) - 0.0095*(***bake temperature***) + 14.27*(***aspect ratio***) + 0.250*(***shape integer = 1)***

Coefficients for normalized area (um)

Category	*Intercept*	*log_{10}(bake time(s))*	*Temperature (C)*	*Vertical aspect ratio*	*Shape Integer*
1	8.50	-0.27	-0.0095	14.27	0.250
2	7.93	-0.22	-0.0076	6.52	2.264
3	4.81	0.13	0.032	-33.06	0.498
4	10.14	-0.25	-0.016	-21.16	0.891

Coefficients for final height in um

Category	*Intercept*	*log_{10}(bake time(s))*	*Temperature (C)*	*Vertical aspect ratio*	*Shape Integer*
1	7.44	-0.21	-0.00286	17.08	0.20
2	9.21	-0.31	-9.31E-05	15.44	2.83
3	-11.08	0.63	0.176	-39.60	0.50
4	17.04	-0.14	-0.0237	-40.66	1.08

Coefficients for lobe height offset (um)

Category	*Intercept*	*log_{10}(bake time(s))*	*Temperature (C)*	*Vertical aspect ratio*	*Shape Integer*
1	0.80	0.047	0.0023	-12.34	0.0421
2	0.002	0.00064	1.741E-05	-0.012	-0.0015
3	1.38	0.039	-0.00719	-1.029	-0.255
4	0.022	-0.00013	-0.00010	0.0544	0.0062

Coefficients for lobe position (um)

Category	*Intercept*	*log_{10}(bake time(s))*	*Temperature (C)*	*Vertical aspect ratio*	*Shape Integer*
1	-136.28	10.72	1.35	-199.23	0.84
2	147.50	1.43	0.24	-2032.69	4.75
3	-4.41	3.83	0.27	-150.20	2.59
4	52.11	-0.50	-0.0027	-207.04	1.24

Coefficients for contact angle (degrees)

Category	*Intercept*	*log_{10}(bake time(s))*	*Temperature (C)*	*Vertical aspect ratio*	*Shape Integer*
1	57.85	-2.05	-0.27	61.99	0.056
2	14.90	-0.25	-0.080	233.45	4.32
3	52.30	8.88	-0.19	-55.70	-7.74
4	31.67	0.13	-0.040	17.52	0.92

3. Surface plots of final parameters v/s process conditions for resist reflow

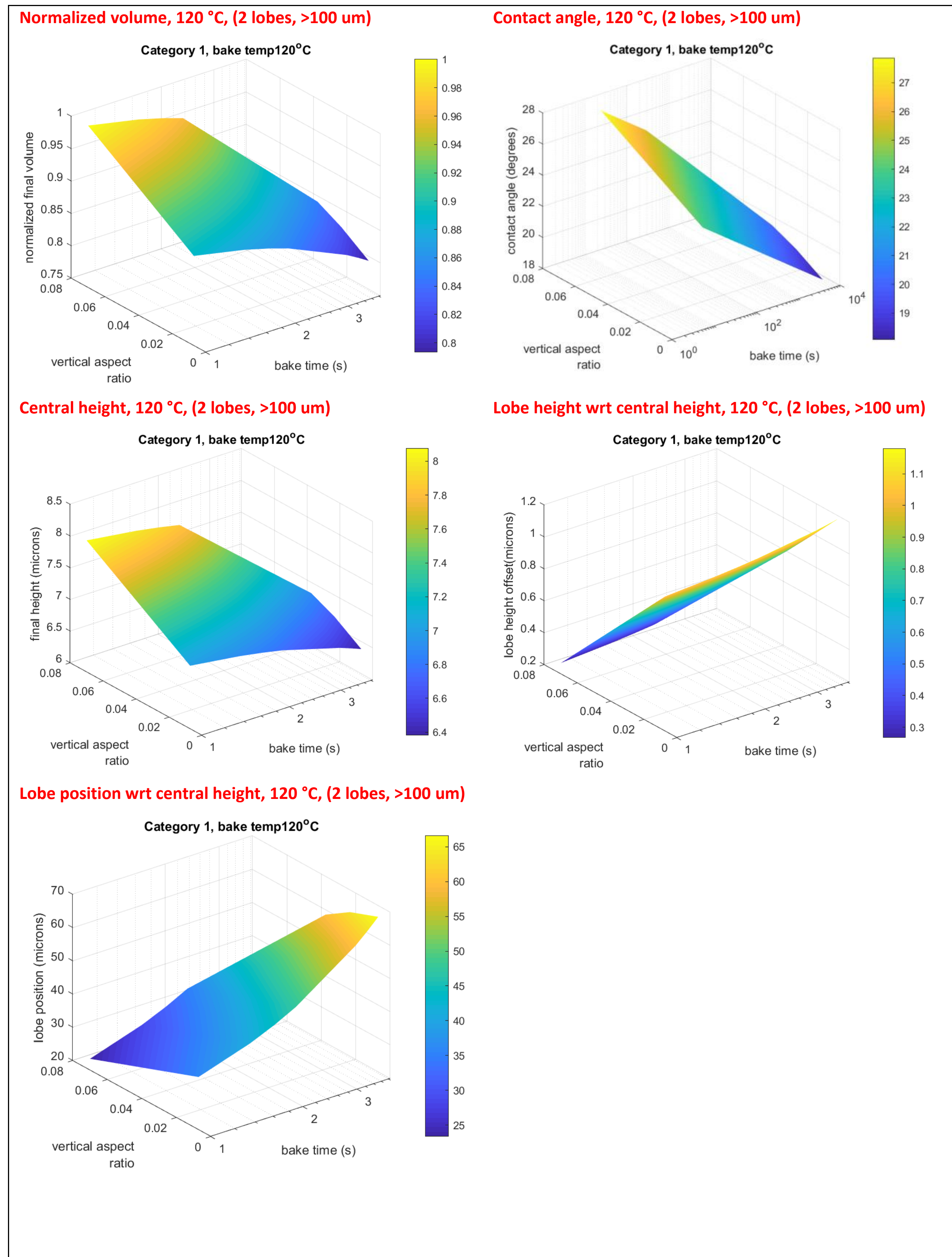

Normalized volume, 120 °C, (1 lobe, >100 um)

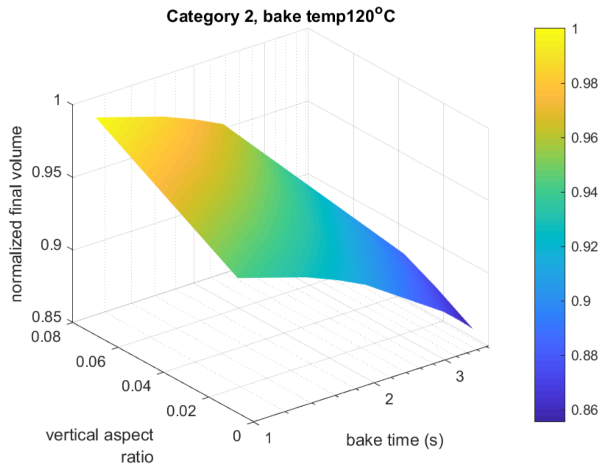

Contact angle, 120 °C, (1 lobe, >100 um)

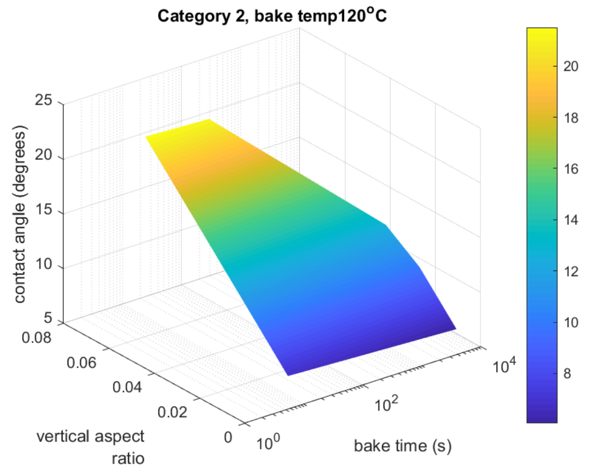

Central height, 120 °C, (1 lobe, >100 um)

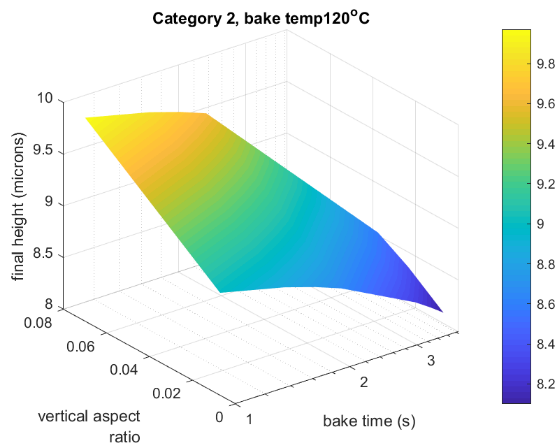

Normalized volume, 120 °C, (2 lobes, <100 um)

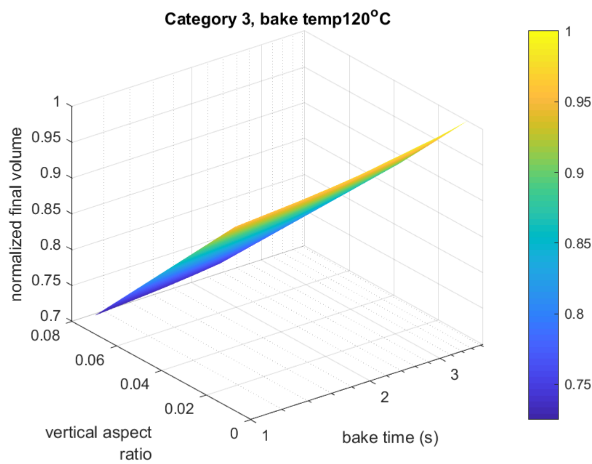

Contact angle, 120 °C, (2 lobes, <100 um)

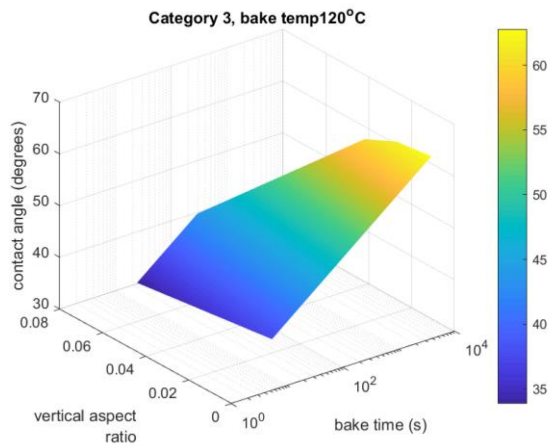

Central height, 120 °C, (2 lobes, <100 um)

Lobe height wrt central height, 120 °C, (2 lobes, <100 um)

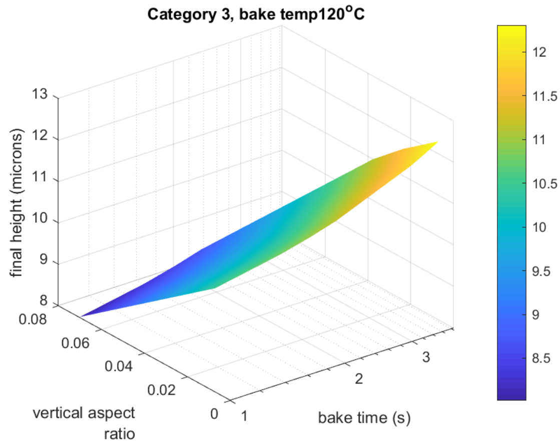

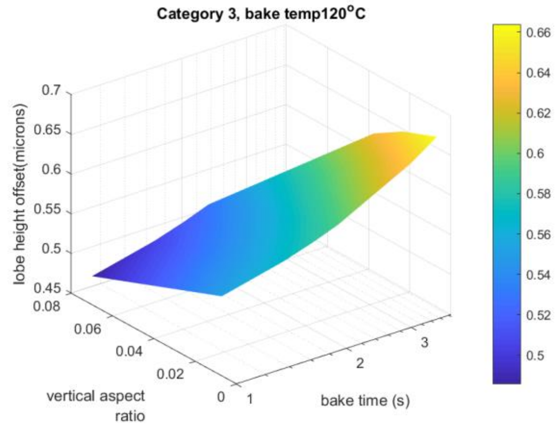

Lobe position wrt central height, 120 °C, (2 lobes, <100 um)

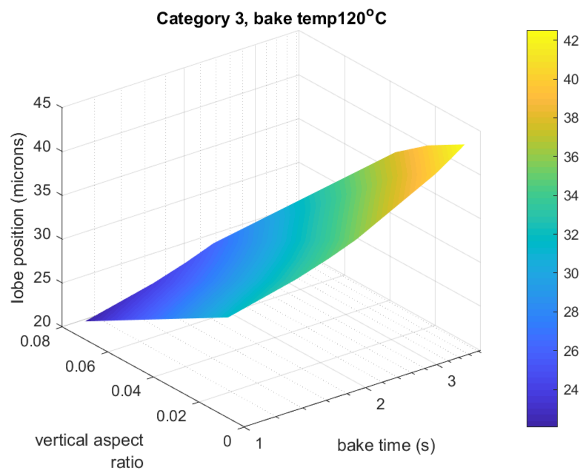

Normalized volume, 120 °C, (1 lobe, <100 um)

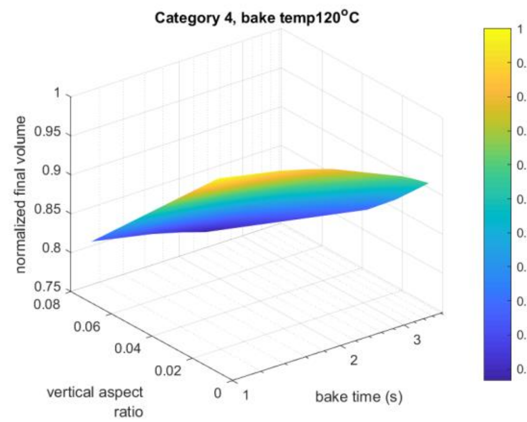

Contact angle, 120 °C, (1 lobe, <100 um)

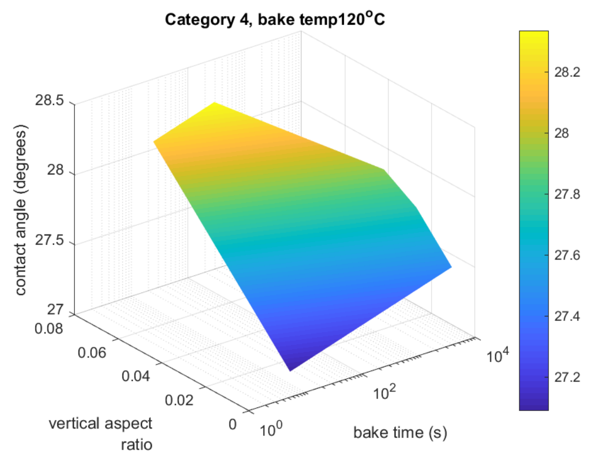

Central height, 120 °C, (1 lobe, <100 um)

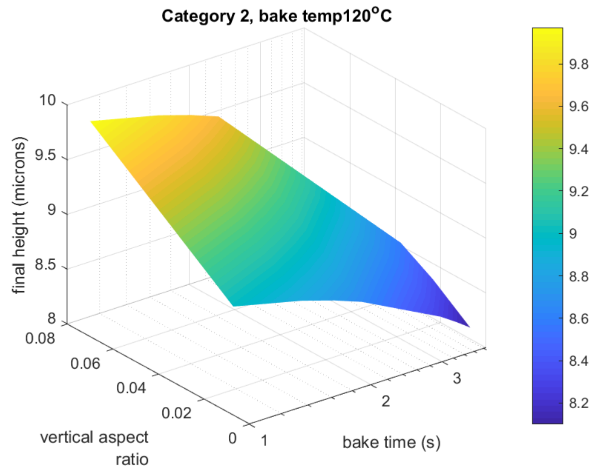

Normalized volume, 140 °C, (2 lobes, >100 um)

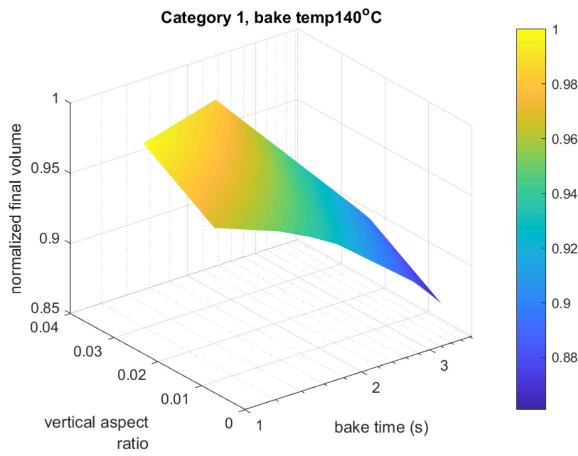

Contact angle, 140 °C, (2 lobes, >100 um)

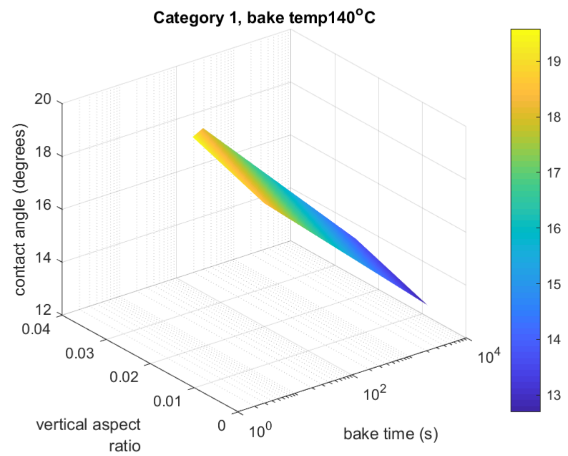

Central height, 140 °C, (2 lobes, >100 um)

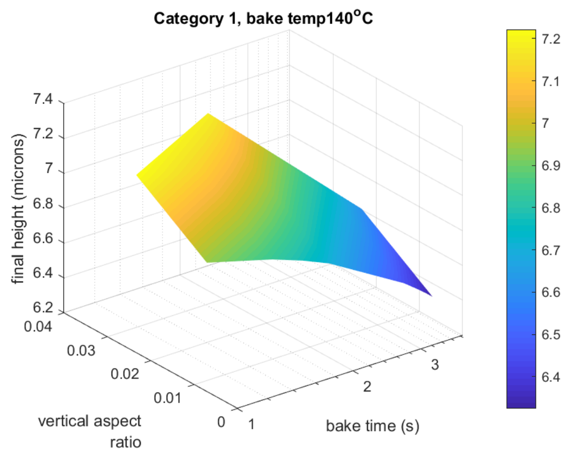

Lobe height wrt central height, 140 °C, (2 lobes, >100 um)

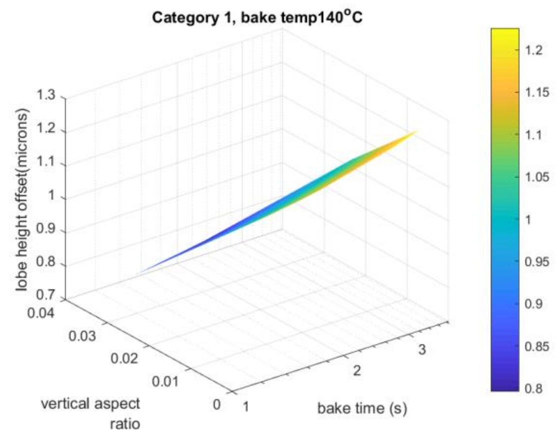

Lobe position wrt central height, 140 °C, (2 lobes, >100 um)

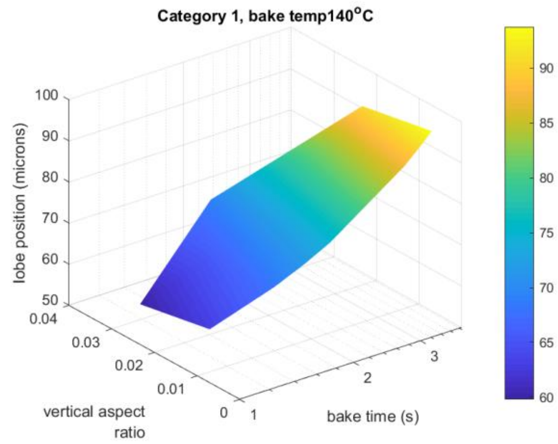

Normalized volume, 140 °C, (1 lobe, >100 um)

Contact angle, 140 °C, (1 lobe, >100 um)

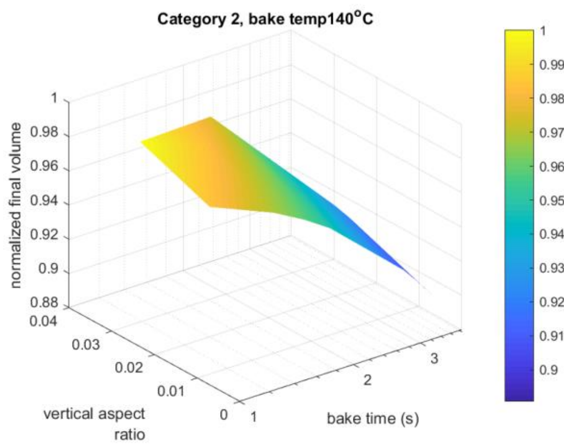

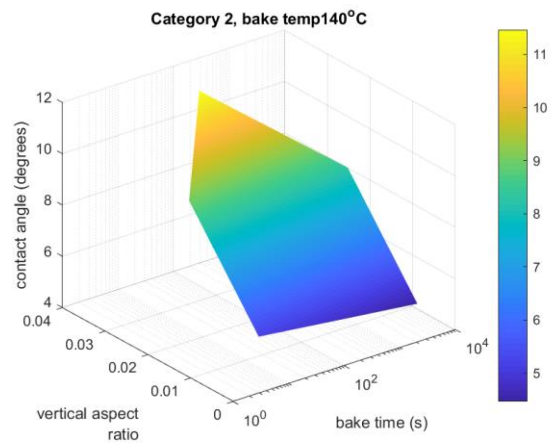

Central height, 140 °C, (1 lobe, >100 um)

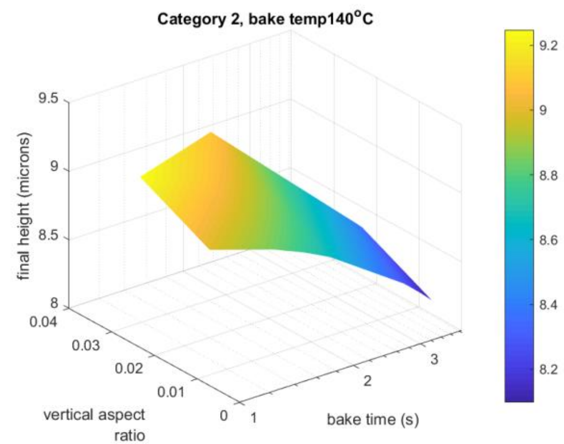

Normalized volume, 140 °C, (2 lobes, <100 um)

Contact angle, 140 °C, (2 lobes, <100 um)

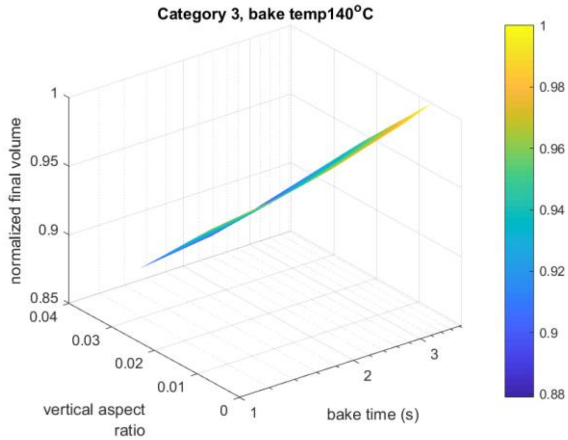

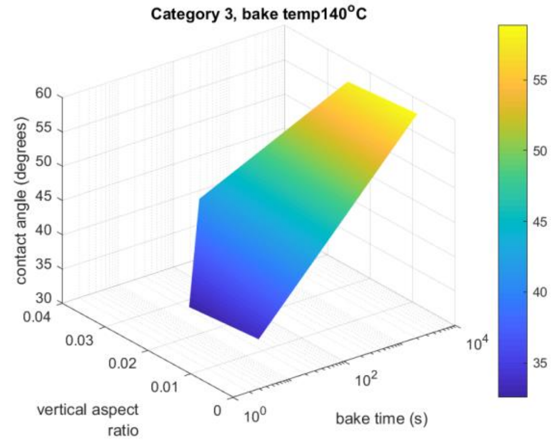

Central height, 140 °C, (2 lobes, <100 um)

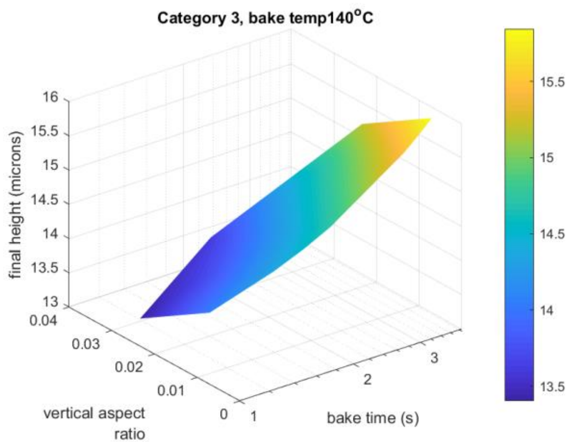

Lobe height wrt central height, 140 °C, (2 lobes, <100 um)

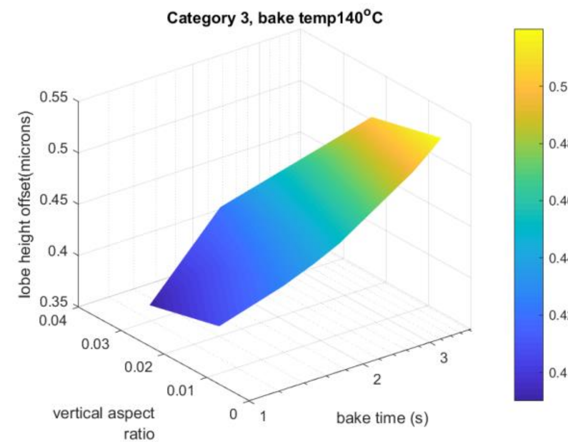

Lobe position wrt central height, 140 °C, (2 lobes, <100 um)

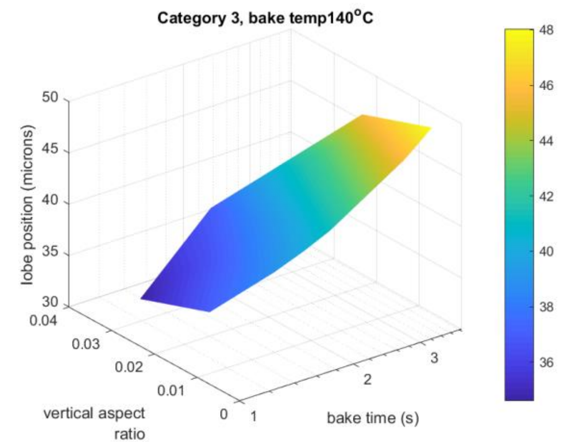

Normalized volume, 140 °C, (1 lobe, <100 um)

Contact angle, 140 °C, (1 lobe, <100 um)

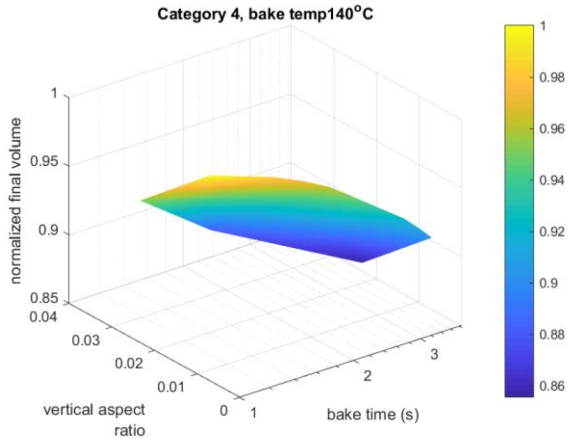

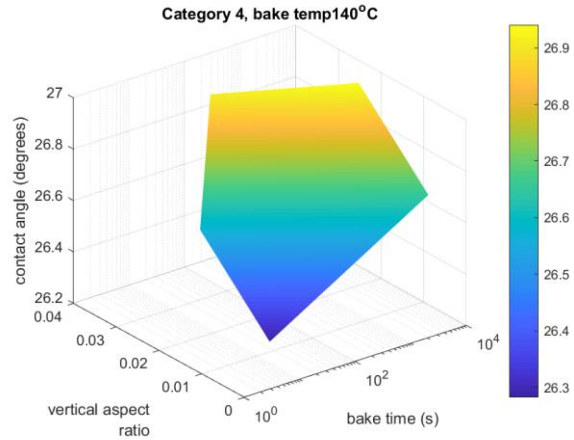

Central height, 140 °C, (1 lobe, <100 um)

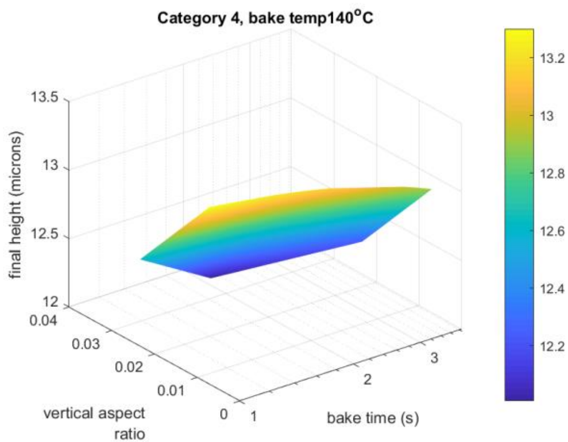

Normalized volume, 180 °C, (2 lobes, >100 um)

Contact angle, 180 °C, (2 lobes, >100 um)

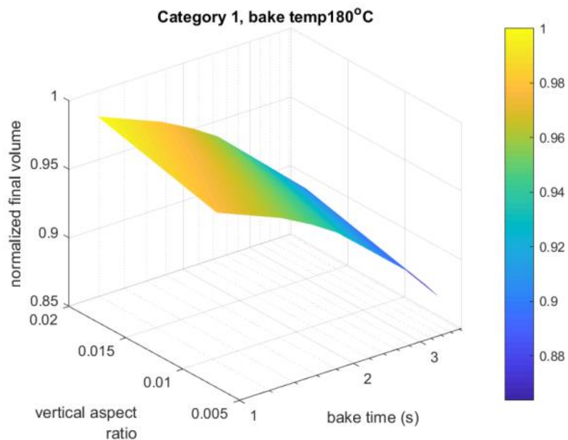

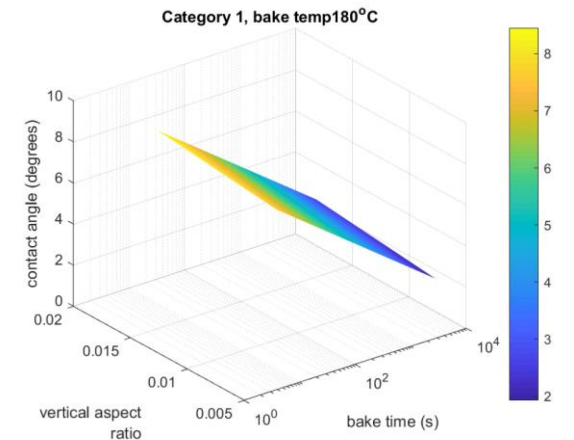

Central height, 180 °C, (2 lobes, >100 um)

Lobe height wrt central height, 180 °C, (2 lobes, >100 um)

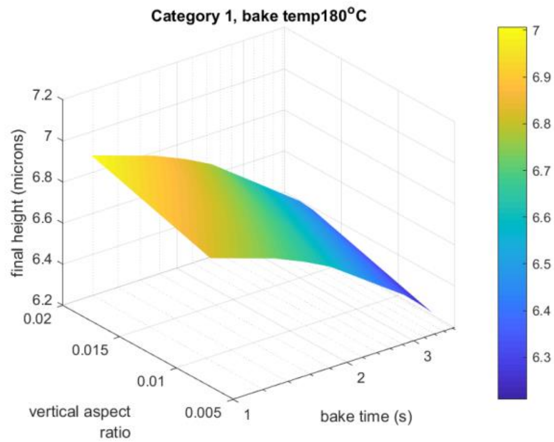

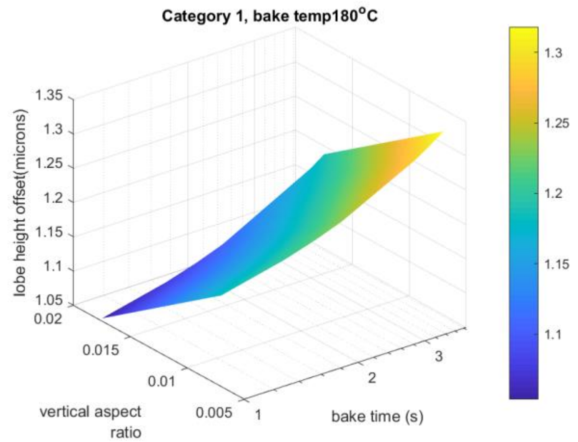

Lobe position wrt central height, 180 °C, (2 lobes, >100 um)

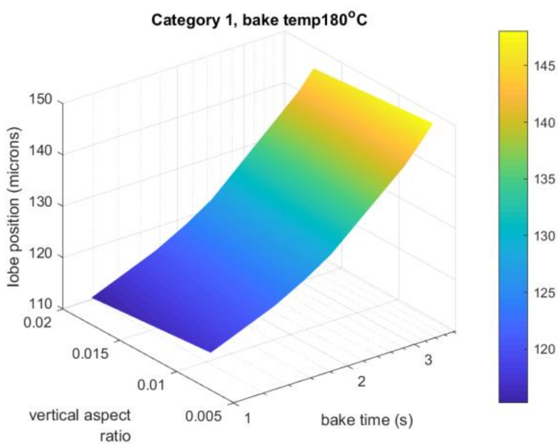

Normalized volume, 180 °C, (1 lobe, >100 um)

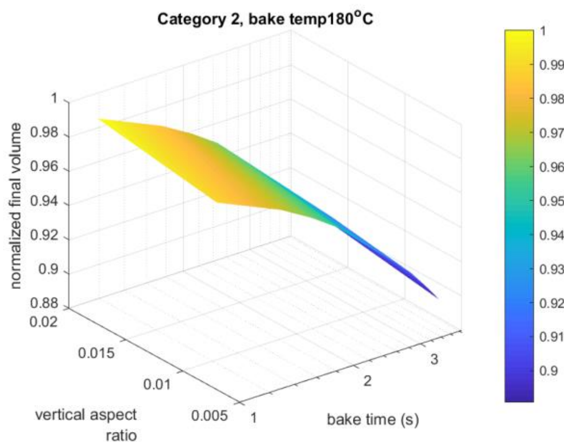

Contact angle, 180 °C, (1 lobe, >100 um)

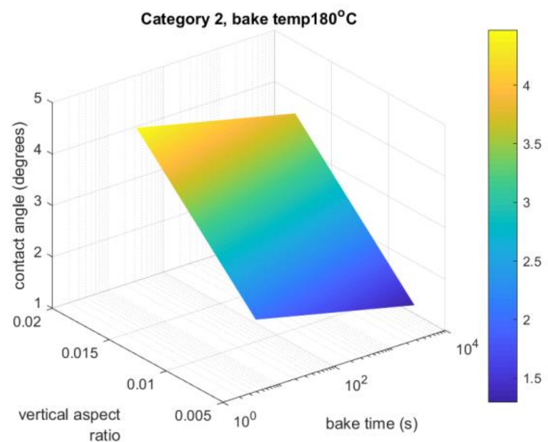

Central height, 180 °C, (1 lobe, >100 um)

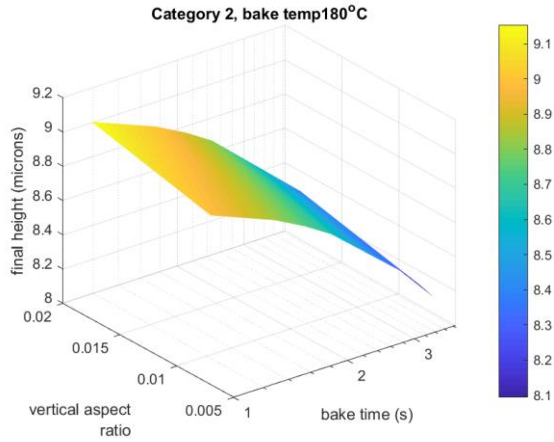

Normalized volume, 180 °C, (2 lobes, <100 um)

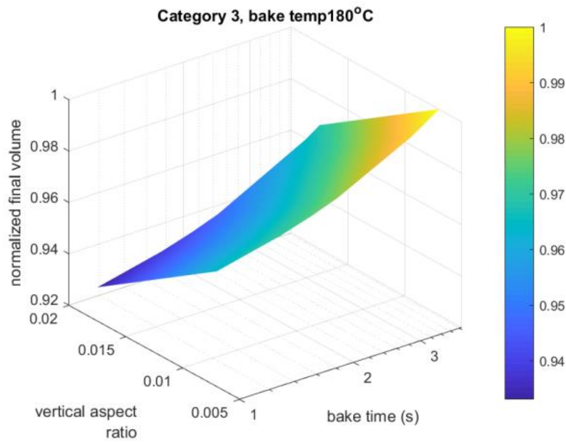

Contact angle, 180 °C, (2 lobes, <100 um)

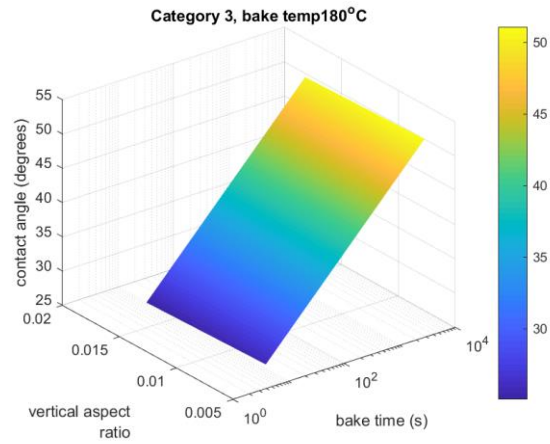

Central height, 180 °C, (2 lobes, <100 um)

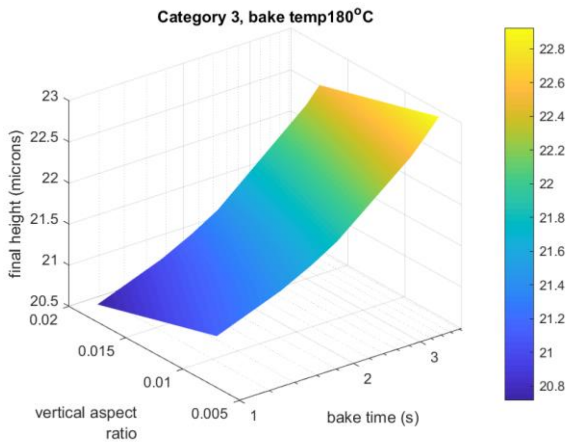

Lobe height wrt central height, 180 °C, (2 lobes, <100 um)

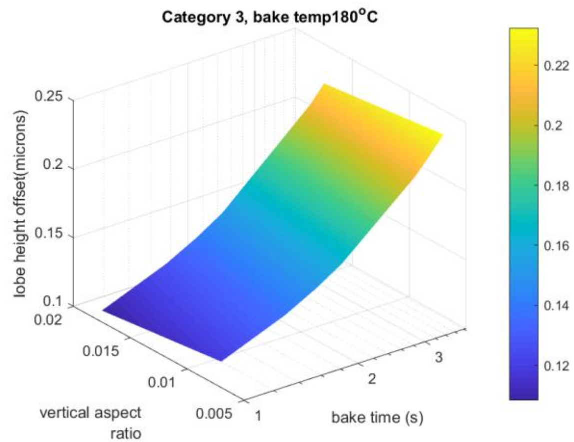

Lobe position wrt central height, 180 °C, (2 lobes, <100 um)

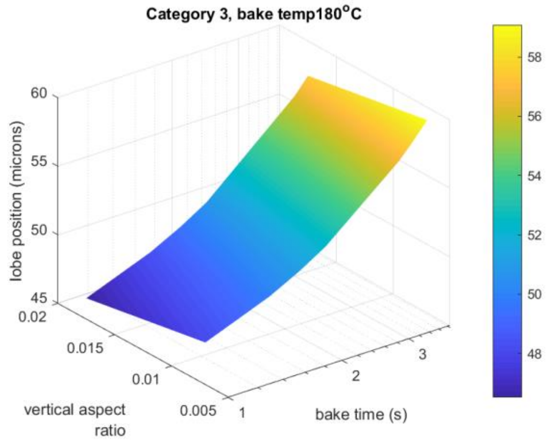

Normalized volume, 180 °C, (1 lobe, <100 um)

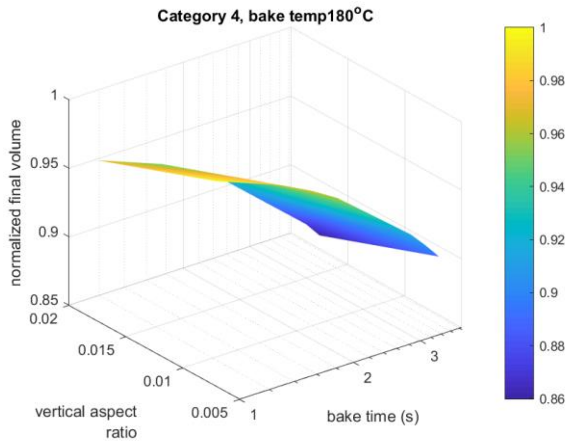

Contact angle, 180 °C, (1 lobe, <100 um)

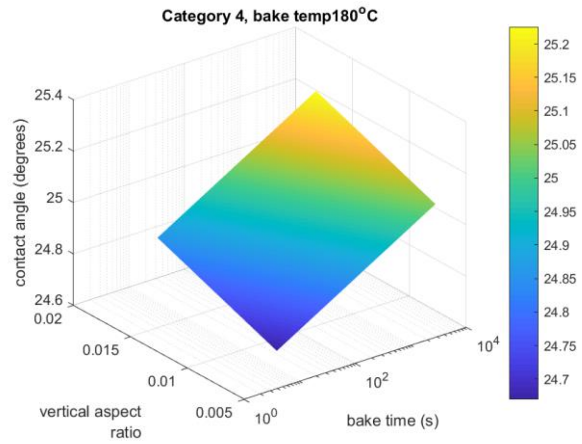

Central height, 180 °C, (1 lobe, <100 um)